ANL-HEP-TR-91-60

HIGH ENERGY PHYSICS DIVISION SEMIANNUAL REPORT OF RESEARCH ACTIVITIES

January 1, 1991 – June 30, 1991

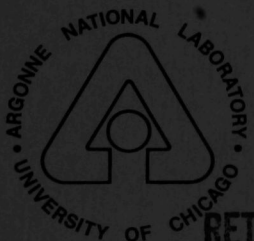

ARGONNE NATIONAL LABORATORY
Argonne, Illinois
Operated by THE UNIVERSITY OF CHICAGO for the
U.S. DEPARTMENT OF ENERGY
under Contract W-31-109-Eng-38

Argonne National Laboratory, with facilities in the states of Illinois and Idaho, is owned by the United States government, and operated by The University of Chicago under the provisions of a contract with the Department of Energy.

Reproduced from the best available copy.

Available to DOE and DOE contractors from the
Office of Scientific and Technical Information
P.O. Box 62
Oak Ridge, TN 37831
Prices available from (615) 576-8401, FTS 626-8401

Available to the public from the
National Technical Information Service
U.S. Department of Commerce
5285 Port Royal Road
Springfield, VA 22161

ANL-HEP-TR-91-60

Argonne National Laboratory
9700 South Cass Avenue
Argonne, IL 60439

HIGH ENERGY PHYSICS DIVISION SEMIANNUAL REPORT OF RESEARCH ACTIVITIES

January 1, 1991 - June 30, 1991

Prepared from information gathered and edited by
the Committee for Publications and Information:

Members: P. Schoessow
P. Moonier
R. Talaga
R. Wagner

August 1991

Table of Contents

ABSTRACT

This report describes the research conducted in the High Energy Physics Division of Argonne National Laboratory during the period of January 1, 1991 - June 30, 1991. Topics covered here include experimental and theoretical particle physics, advanced accelerator physics, detector development, and experimental facilities research. Lists of division publications and colloquia are included.

I. EXPERIMENTAL PROGRAM

A. Physics Results

1. CDF Physics

Data analysis has continued on electroweak and QCD studies using the 1988-89 data. Papers are in various stages of completion (e.g., submitted for publication or under review by the collaboration) on: (a) inclusive W and Z-boson production; (b) electroweak asymmetry in Z production and decay; (c) QCD asymmetry in W production; (d) Limits on new W' and Z' boson masses; (e) inclusive jet production and compositeness; (f) high p_T prompt photon production; (g) b production and $b\bar{b}$ mixing. This is a partial but representative list of topics. We summarize the status of these efforts as follows.

a) W and Z Production

The total cross sections for W and Z production, using the central electron data set, have been accepted for publication in Physical Review. The inclusive W p_T spectrum, again based on the central electron data set, has been published in Physical Review Letters; the corresponding inclusive Z p_T spectrum, based on both the central electron and central muon data sets, has been submitted to Physical Review Letters. These data all show excellent agreement with next-to-leading order (NLO) QCD predictions. Using the central electron and muon data sets, CDF has also set limits on the masses of possible W' and Z' vector bosons with standard model couplings to quarks and leptons, namely:

$$M(W') > 520 \text{ GeV (95\% CL.)}$$
$$M(Z') > 412 \text{ GeV (95\% CL.)}$$

Current particle data group limits are 220 and 180 GeV respectively for W' and Z' masses.

b) Electroweak Asymmetries

CDF has submitted for publication a measurement of the electroweak asymmetry in Z^0 decay, from the central electron data set. This asymmetry is sensitive to the weak current vector-axial vector interference term in the process $q\bar{q} \rightarrow Z^0 \rightarrow e^+e^-$. The result, expressed in terms of the weak mixing angle,

$$\sin^2 \bar{\theta} = 0.228 \pm 0.017$$

is consistent with more precise determinations by the LEP experiments ($\sin^2 \overline{\theta} = 0.2323 \pm 0.0014$, from recent global analyses of combined LEP measurements). CDF has also measured the QCD asymmetry in production of W^+ and W^- bosons; this asymmetry is sensitive to the valence quark content of the initial state proton and antiproton, and is reflected in a boosted rapidity distribution for W^+ (W^-) along the proton (antiproton) beam directions. Figure 1 shows the resulting lepton asymmetry distributions for the central electron and muon samples, compared with leading order QCD predictions for a variety of structure functions.

c) High p_T Jet Production

Figure 2 shows the inclusive single jet production in the central region, compared with NLO predictions by Ellis, Kunszt and Soper, using MRSB structure functions; (a) shows the p_T dependence on a log scale, extending over more than 10 decades in cross section, while (b) shows the ratio of observed cross section to NLO theory, out to $p_T >$ 400 GeV/c. The low p_T region ($p_T < 20$ GeV/c) has been augmented using a set of minimum bias triggers. From the overall p_T dependence, we can set a lower limit, $\Lambda_c >$ 1400 GeV, on the compositeness scale. This value may be compared with previous limits of 700 GeV (CDF, 1987) and 825 GeV (UA2, 1990). We also confirm the qualitative dependence of jet cross section on cluster cone size, predicted by NLO QCD.

d) Prompt Photon Production

The cross section for single prompt photon production has been measured using the photon shower profile (at shower max.) to separate single photons from multiple photon backgrounds (e.g., π^o's, η's, $K_s \rightarrow \pi^o \pi^o$, etc.). The shower profile systematics are based on electron shower data from the test beam and from the W and Z^o electron samples. In addition, CDF has used the 10 GeV electromagnetic cluster trigger sample to obtain direct measurements of inclusive high p_T π^o and η production. Figure 3 shows the mass spectrum for photon pairs identified in the shower max. detector in the central calorimeter; the minimum separation for these pairs is 5 cm (20 cm) for π^o's (η's). The background under the visible π^o and η peaks arises from both multiple π^o production and misidentified single photon showers. Due to the larger minimum separation, the η peak provides a clean source of single photon showers, which can be used to calibrate the shower profile response. This is shown in Fig. 4, where the photons from the η mass peak (4a) are fitted to a single photon shower profile in order to extract a fit χ^2 (4b). The Monte Carlo prediction, based on electron shower data, agrees well with the observed single photon χ^2 distribution. The π^o's, because of the much smaller minimum separation, provide a source

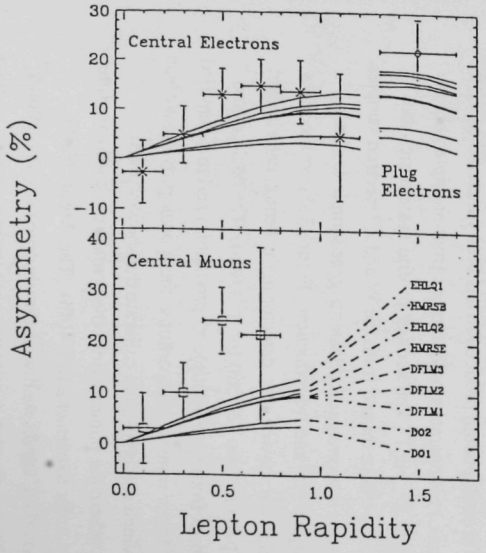

Fig. 1. Lepton asymmetries in W events compared to predictions of leading-order calculations for various parton distributions.

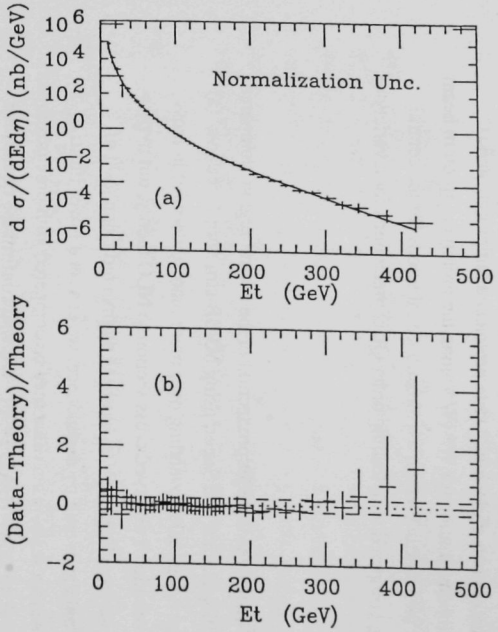

Fig. 2. Inclusive jet production cross section compared with NLO predictions (a); ratio of observed to theoretical cross section for MRSB structure functions (b).

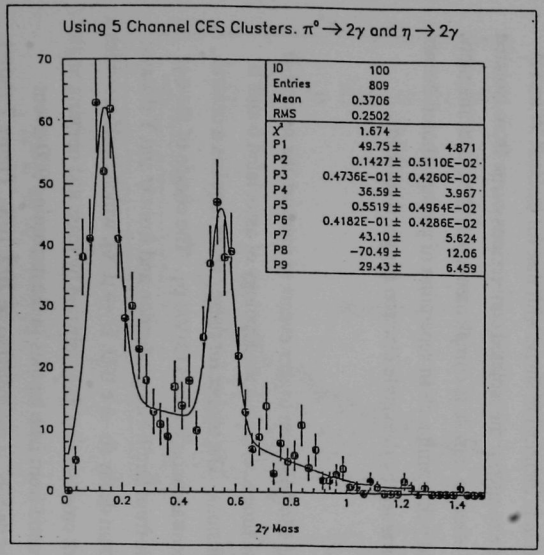

Fig. 3 Two photon mass distribution from $E_T > 10$ GeV EM cluster trigger sample, using a 3-channel cluster algorithm in the shower max. detector to improve the efficiency for π^0s.

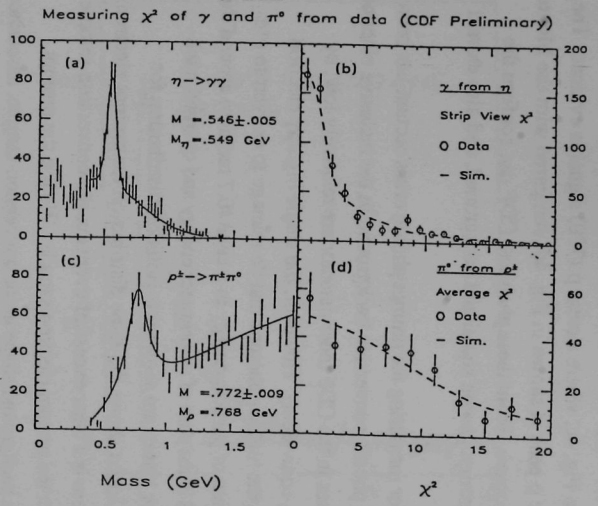

Fig. 4. (a) Two photon mass spectrum, using standard 11-channel cluster algorithm in shower max. detector; (b) shower profile chisquare for single photons from eta decays (points), compared with shower simulation; (c) mass spectrum for EM clusters with single charged tracks, using standard 11-channel shower max. clustering; (d) shower profile χ^2 for π^0's (from background subtracted ρ peak), compared with monte carlo.

of "pure background", that is, overlapping photon showers. The invariant mass of the π°'s with charged tracks is shown in Fig. 4c, where a clear ρ (770) signal is evident. The shower profile χ^2 for the π°'s in the ρ peak is shown in Fig. 4d, compared with the Monte Carlo prediction for overlapping showers. From these analyses, CDF can confirm the shower profile predictions for the prompt photon signal and background, and also extract the η to π° cross section ratio.

A complementary method for measuring the prompt photon cross section has been developed, which makes use of the photon conversion background in the inclusive electron data set. The photon conversion rates in the CDF inner detector are relatively low, by design (the inner detector is 5% X_0 equivalent). However, the single high p_T electron trigger is very efficient in detecting the high p_T photons that do manage to convert to e^+e^- pairs. Figure 5 shows the distribution of particle energy in a cone (0.7 radians) around the trigger electron; the variable plotted is the sum of calorimeter energy and charged track momenta, added in quadrature. The histogram shows this isolation distribution for conversion pairs, while the shaded insert shows the same distribution for prompt electrons in QCD jets (e.g., b, c, $\rightarrow e^{\pm}$). There is a clear excess of events in the conversion sample that are "isolated" as compared with the prompt electron sample. We use the prompt electron distribution to estimate the background shape in the conversion sample, associated with conversion photons in QCD jets. After subtracting this background, normalized on the high side of Fig. 5, we obtain the isolation variable distribution for prompt photons in Fig. 6 (solid points); this distribution is identical in shape with that for isolated W and Z electrons (histogram in Fig. 6), as expected if the isolated conversions come from isolated prompt photons. The conversion electron sample is complementary to the electromagnetic cluster trigger sample in CDF, and will permit a clean separation of prompt photon events down to x_T values of 0.008 (determined by the single electron trigger threshold).

e) Bottom Production

CDF has used a sample of 1340 dilepton trigger events to measure the neutral-B mixing parameter, and at the same time to establish the topology of associated b and $\overline{b}$ production in high p_T hadron collisions. The trigger for these events requires a central electron above 5 GeV E_T and a central muon above 3 GeV/c p_T. The choice of the e-μ final state eliminates backgrounds from Drell-Yan production and from ψ and Y decays. Background from sequential bottom decay ($b \rightarrow e\, \upsilon\, D$, $D \rightarrow \mu\, X$), which itself provides a useful check on the single b-quark cross section, is eliminated by mass and opening angle cuts on the e-μ pair. The background from fake leptons in the remaining 900-event sample, after removing sequential decays, is estimated to be $20 \pm 10\%$. Figure 7 shows

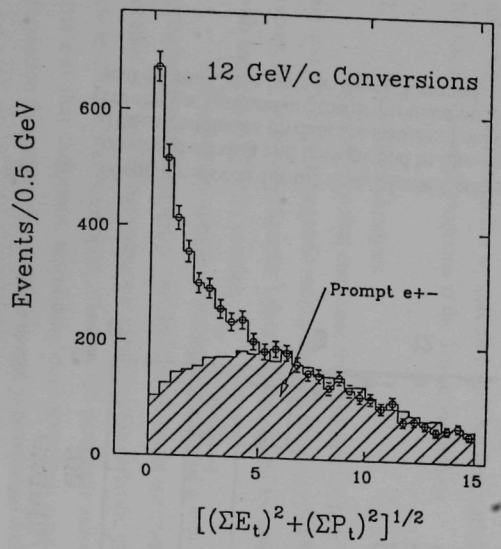

Fig. 5. Distribution of isolation variable, defined as sum of calorimeter and charged track energy in a cone of radius 0.7, added in quadrature, for all conversion pairs (histogram), and prompt electrons from b,c jets (shaded insert); the latter have been scaled to match the conversion spectrum for large values of the isolation variable.

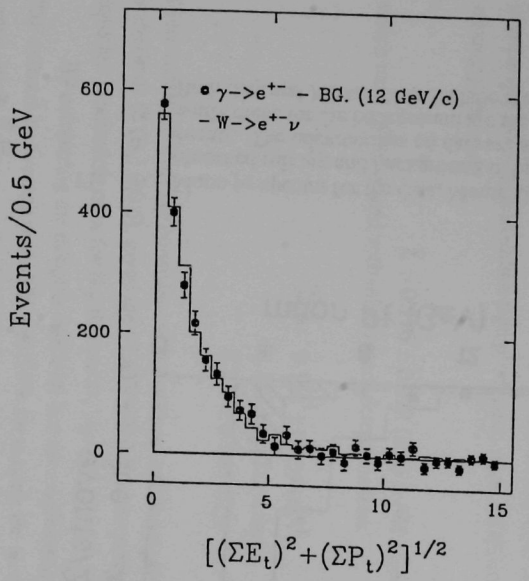

Fig. 6. Isolation distribution for conversion pairs after background subtraction (points), and for $W \rightarrow e\pm$ decays (histogram).

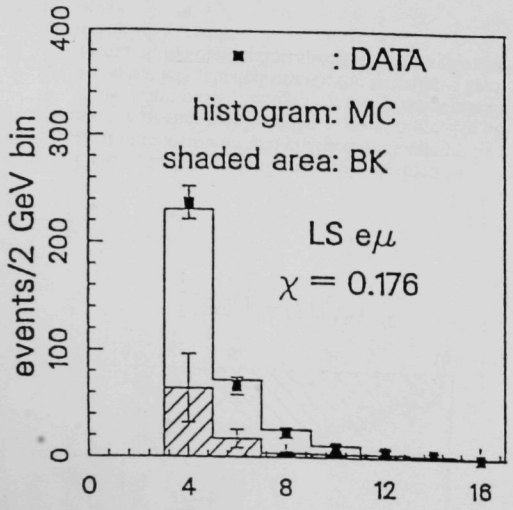

Fig. 7a. Muon p_T spectra for the data, Monte Carlo with the observed mixing and background in like-sign eμ events. The uncertainties on data are statistical only, while those for the background are the determined 50%. Both data and Monte Carlo include the background.

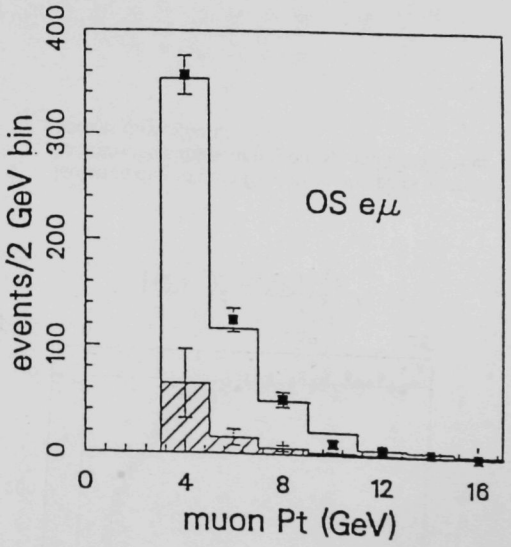

Fig. 7b. Muon p_T spectra for the data, Monte Carlo with the observed mixing and background in opposite-sign eμ events. The uncertainties on data are statistical only, while those for the background are the determined 50%. Both data and Monte Carlo include the background.

the muon p_T spectrum for like-sign and unlike sign events, together with the fake lepton background contribution and the Monte Carlo prediction with mixing. The p_T dependence is in good agreement with the Monte Carlo. Roughly half of the like sign rate can be ascribed to mixing, the other half to fake muon background and $b \rightarrow c \rightarrow$ lepton. By comparing like sign and unlike sign production rates, CDF obtains a species average mixing parameter.

$$\overline{\chi} = 0.176 \pm 0.028 \text{ (stat)} \pm 041 \text{ (syst.)},$$

which may be compared with other recent determinations,

$$\begin{aligned} \overline{\chi} = \quad & 0.158 \pm 0.059 \text{ (UA1)} \\ & 0.132 \pm 0.027 \text{ (Aleph)} \\ & 0.178 \pm 0.045 \text{ (L3)} \end{aligned}$$

These measurements are consistent with the Standard Model prediction that $B_s - \overline{B_s}$ mixing is maximal (χ (B_s) = 0.5), given the CLEO/ARGUS measurements on χ (B_d) and the expected production rates for B_u, B_d, and B_s mesons.

By comparing the dilepton rate with that for single lepton production from b's, CDF extracts an average probability of 0.4% for tagging the second b (using a 3 GeV/c muon), given a trigger on the first b (using a 5 GeV electron). This rate is obviously much lower than the semileptonic branching ratio (11.5%), and reflects the fact that the topology for $b\bar{b}$ production at a hadron collider is not back-to-back. Typically the second b-quark in an event has a much softer p_T spectrum than the first, and this has important implications for future b-physics programs at the Tevatron Collider (A. B. Wicklund)

2. Soudan Data Analysis

Argonne physicists continued their activities in four areas of Soudan data analysis: the search for GUT magnetic monopoles, the identification of contained neutrino interaction events, the analysis of Soudan 1 data, and the search for underground muons associated with astrophysical point sources.

The search for magnetic monopoles suffered a setback at the end of 1990, when it appeared that its completion would have to await the reprocessing of all past raw data because of a flaw in the monopole identification software used until then. In early 1991 a new technique was developed, allowing the monopole search to proceed immediately. It turns out that the muon astronomy data summary tapes contain enough ionization information for monopole candidate events to be selected with high efficiency. About 3000

track-like events with high ionization were identified in this way, and the raw data for these events are now being extracted from the data tapes. Scanning of these events is very fast because their high ionization is nearly always caused by obvious showers or delta rays. True GUT monopoles should have uniformly heavy ionization, and should not produce delta rays for monopole velocities $\beta < 0.95$. By the end of June most of the monopole candidate events had already been extracted and scanned. A Monte Carlo simulation of the new procedure showed it to have high efficiency for monopole tracks. It is planned to complete the analysis and report the results in a journal article during the second half of 1991.

The Soudan 2 contained event sample includes cosmic-ray (atmospheric) neutrino and neutron interactions as well as nucleon decay candidates. The interactions of atmospheric neutrinos are a background to nucleon decay, but can also be used to search for neutrino oscillations through the ν_μ/ν_e ratio. The interactions of low-energy neutrons, produced by cosmic-ray muon showers in the rock surrounding Soudan 2, are identified by hits in the active shield as well as by topology and ionization. Comparisons of neutron and neutrino candidate events with Monte Carlo simulations provide valuable checks on the performance of the detector. During the past two years, contained events have been selected by software filters which have improved substantially over that period. It has therefore been planned for some time to reprocess all past Soudan 2 data using the latest offline software. After nearly a year of preparation, the reprocessing began in early May, using improved track reconstruction algorithms, the latest survey data, and new filters for contained events, semi-contained events, and multiple muon events.

The reprocessing is being performed on the large VAX clusters at the University of Minnesota and the Rutherford Laboratory. Argonne physicists worked on the development of the new contained event filter software and of higher level filters to select neutrino and neutron candidate events from the reprocessing output files. The loosest possible cuts are applied in the primary filter, so that changes in event selection can be made with the higher level filters to study biases and efficiencies. Until now the initial filter cuts were quite restrictive, and their biases could be studied only through Monte Carlo simulations. The new filter also uses a 25% larger fiducial mass, with a corresponding increase in the number of contained events. During May and June much effort was devoted to studying the first samples of contained events from the reprocessing, and to developing higher level filters which reject background and select neutrino, neutron, and nucleon decay candidate events with high efficiency. The reprocessing is expected to be completed in the Fall of 1991.

Argonne physicists also continued to work on the analysis of data from the Soudan 1 experiment. These efforts focussed on the search for evidence of underground muons associated with Cygnus X-3 through the development of new statistical methods. The original analysis of muons from the direction of Cygnus X-3 was performed at the University of Minnesota, and is being independently repeated, checked, and extended at Argonne. Argonne physicists also worked on the interpretation of surface-underground coincidence data from Soudan 1 and its surface air-shower array, to obtain information about the nuclear composition of the cosmic ray primaries. The surface array provides a measure of the energies of primaries which produce multiple muon events in the underground detector. As described below, the operation of a similar surface air shower-array in coincidence with Soudan 2 has just begun.

The idea that astrophysical objects, such as the X-ray binary Cygnus X-3, might be observable in the underground muon flux has continued to fascinate Soudan physicists since initial evidence from the Soudan 1 detector was published in 1985. On two nearby days during the Cygnus X-3 radio flare of January 1991, Soudan 2 recorded a total of 32 muons within 2° of the Cygnus X-3 direction, when 11.4 muons were expected. Figure 8 shows the numbers of muons per day, expected and observed, from the direction of Cygnus X-3. Figure 9 is a scatter plot of number of muons per day observed from the direction of Cygnus X-3 versus the number expected, for each of the 696 days of Soudan 2 data. The two days during the January 1991 flare stand out quite clearly. However, no excess muon flux is observed during any of the other four Cygnus X-3 radio flares which occurred during the 2-year period for which Soudan 2 has data. The probability that the excess muon flux observed arises from a fluctuation of the background rate is estimated to be between 5% and 0.05%. Although the effect seems unlikely to be a statistical fluctuation, confirmation will only be provided by other experiments and by future observations of radio flares.

In addition to writing a number of internal PDK notes during the first half of 1991, Argonne physicists also coauthored several external documents submitted by the Soudan 2 collaboration. Most notable among these are the Fermilab long baseline neutrino oscillation proposal (P-822), contributions to the conceptual design report for the Fermilab main injector neutrino program, and the paper on Protheroe's statistic and continuous distributions (published in Nuclear Instruments and Methods in Physics Research). Argonne physicists were coauthors on a paper analyzing intranuclear rescattering rates for low energy pions created within neon nuclei by muon-neutrino interactions (submitted to Physical Review D), and on nine abstracts submitted to the 22nd International Cosmic Ray Conference (to be held in Dublin in August 1991). One Ph.D. thesis was submitted by

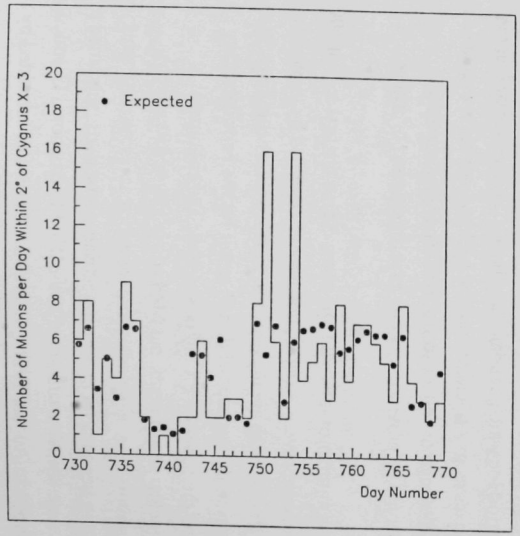

Fig. 8. The number of muons detected by Soudan 2 within a 2° half-angle cone centered on Cygnus X-3 versus calendar day number. Days 750 and 753 are 20th and 23rd January 1991 (CST) respectively. The superimposed points are the expected numbers of muons, which depend on the livetime of the detector on each day.

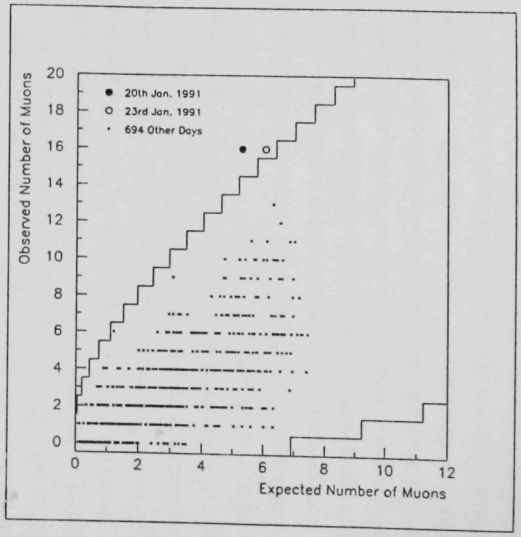

Fig. 9. A scatter plot of the number of muons observed by Soudan 2 from the direction of Cygnus X-3 on a given day versus the number expected on that day, for a total of 696 days. The lines show the 10^{-3} probability boundaries.

Soudan 2 graduate student Mark Lowe (University of Minnesota) on the search for astrophysical point sources of underground muons. (D. Ayres)

3. E609 Collaboration

During this period, our new experimental results which show clear evidence for substantial nuclear scattering of the outgoing scattered partons were published (Phys. Lett. 259, 209 (1991)). These data also show that the angular width of the individual scattered jets is only slightly affected by the presence of the nucleus. This latter result would be expected from the usual (uncertainty principle) argument which indicates that most of the parton fragmentation process takes place after the scattered parton has emerged from the nucleus. An important practical implication of this approximately constant jet angular width is that the large scattering angles of the observed secondary scattering are unlikely to have been affected by systematic experimental errors.

When taken together with our earlier published observation of a large energy loss of high energy partons traversing nuclei (~ 3 GeV/Fermi), these results form a picture which is in sharp contrast with the established result that the incident parton in Drell-Yan production from nuclear targets suffers virtually no angular deflection while traversing nuclear matter. The "factorization theorem" in QCD provides a framework for understanding the Drell-Yan result, but its application to hard collisions producing dijets (at comparable or larger values of Q^2 than the Drell-Yan data) is not yet understood in a quantitative way. Another theoretical area for which our results pose a challenge concerns the relationship of the size of the observed secondary parton scattering to the size of the observed anomalous nuclear enhancement.

We are extending our analyses in order to make quantitative studies of the p_T and A dependence of the secondary nuclear scattering. Related goals are to refine our earlier analysis of the anomalous (A^{α}) nuclear enhancement and of the various substantial "k_T" effects in our data. We plan to report these studies and other results in a detailed final E609 paper during the coming year. (T. Fields)

4. Polarized Proton Physics

Activities associated with the polarized proton physics were: i) E-704 data analyses, ii) preparation of the Fermilab polarized-beam proposals, and iii) formation of RSC (RHIC SPIN Collaboration) and study of RHIC detectors. We report only on the first item at this time. E-704 data analyses were carried out for the following measurements:

- Using polarized beams and a hydrogen target, the single-spin asymmetry, A_N, was measured in $p^\uparrow p \rightarrow (\pi^\circ, \eta)X$ and $\bar{p}^\uparrow p \rightarrow \pi^\circ X$ at large p_T as well as $p^\uparrow p \rightarrow (\pi^\circ, \pi^+, \pi^-, \Lambda)X$ and $\bar{p}^\uparrow p \rightarrow (\pi^\circ, \pi^+, \pi^-)X$ at large x_F.

- Using polarized beams and a polarized target, the spin correlation parameter, A_{LL}, was measured in $p^\uparrow p^\uparrow \rightarrow \pi^\circ X$ and $\bar{p}^\uparrow p^\uparrow \rightarrow \pi^\circ X$ as well as $\Delta\sigma_L(pp)$ and $\Delta\sigma_L(\bar{p}p)$, the differences in total cross sections of pure spin states.

While analyses for $\Delta\sigma_L$ and Λ-production data are in progress, we report some results of these measurements.

a) Comparison of $p^\uparrow p \rightarrow (\pi^\circ, \eta)X$ and $\bar{p}^\uparrow p \rightarrow \pi^\circ X$ at large p_T

Data of the $p^\uparrow p$ reaction at 200 GeV/c show that the asymmetry values (A_N) at $x_F \approx 0$ are approximately zero (or slightly negative) up to $p_T = 3.5$ GeV/c and then begin to rise to $\sim +40\%$ in the region of $p_\perp = 4 - 5$ GeV/c as shown in Fig. 10a. At lower energies from 10 to 40 GeV/c, this rapid rise from zero to large positive values was also observed, although none of the data exceeded $p_T = 3$ GeV/c. A new finding is that all the A_N data for π° production at $x_F \approx 0$ show large positive asymmetries beginning at $x_T = 0.4$ in the region $\sqrt{s} = 5 - 20$ GeV. This is strong indication that we are indeed observing asymmetries caused by hard scattering.

Single-spin asymmetry in $\bar{p}^\uparrow p \rightarrow \pi^\circ X$ shows a p_T dependence similar to the $p^\uparrow p$ case. However, data are limited to $p_T \leq 3.5$ GeV/c as shown in Fig. 10b. We have also observed a similar p_T dependence in $p^\uparrow p \rightarrow \eta X$ as shown in Fig. 11.

b) x_F Dependence of Single-Spin Asymmetry in $p^\uparrow p \rightarrow \pi^\circ X$ and $\bar{p}^\uparrow p \rightarrow \pi^\circ X$

Asymmetry measurements (A_N) on the x_F dependence at 200 GeV/c covering p_T up to 2 GeV/c were carried out. A_N values in the $p^\uparrow p$ reaction are consistent with zero up to $x_F = 0.3 - 0.4$, and then linearly increase to $+20\%$ near $x_F = 1.0$ as shown in Fig. 12. This is the first x_F dependence data ever obtained for π production. It is interesting to note that our data resemble the x_F dependence for Λ polarization in $pp \rightarrow \Lambda^\uparrow X$, where polarized s quarks are considered to be responsible for high polarization.

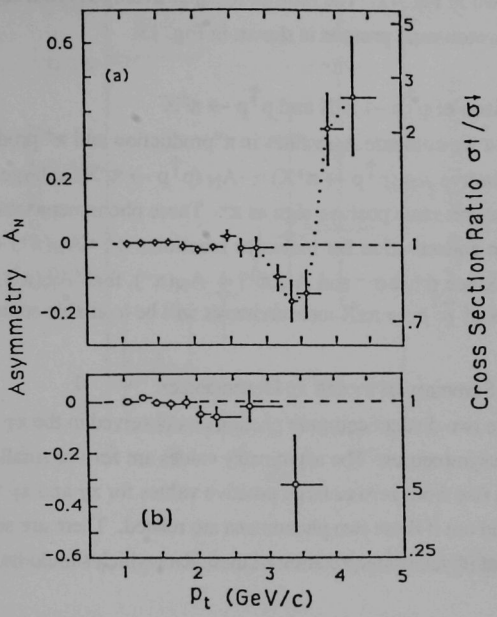

Fig 10 a. p_T dependence of A_N at $x_F \approx 0$ in $p\uparrow p$ reaction.

b. p_T dependence of A_N in $\bar{p}\uparrow p \to \pi^\circ X$.

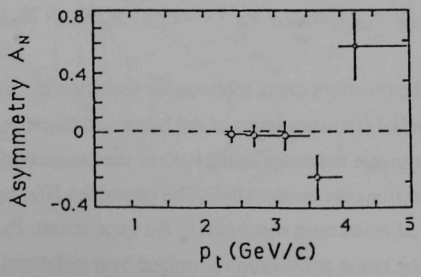

Fig 11. p_T dependence of A_N in $p\uparrow p \to \eta X$.

The single spin asymmetry in $\bar{p}^{\uparrow} p \rightarrow \pi^{\circ} X$ shows a similar x_F dependence to the $p^{\uparrow}p$ case as shown in Fig. 12. The ratio of the spin-averaged cross sections for π° production by antiprotons and protons is shown in Fig. 13.

c) Comparison of $p^{\uparrow}p \rightarrow \pi^{\circ} X$ and $p^{\uparrow}p \rightarrow \pi^{\pm} X$

In Fig. 14 we compare A_N values in π°production and $\pi^{\pm}$ production. It is remarkable to observe $A_N (p^{\uparrow}p \rightarrow \pi^{+}X) = -A_N (p^{\uparrow}p \rightarrow \pi^{-}X)$ at large x_F. Note that $A_N (p^{\uparrow}p \rightarrow \pi^{\circ}X)$ has the same positive sign as π^{+}. These phenomena can be understood by applying isospin conservation for inclusive reactions, $\sigma^{+} \bullet A_N(\pi^{+}) + \sigma^{-} \bullet A_N(\pi^{-}) = 2\sigma^{\circ} \bullet A_N(\pi^{\circ})$. Since $\sigma^{+} < \sigma^{-}$ and $A_N(\pi^{+}) \approx -A_N(\pi^{-})$, then $A_N(\pi^{\circ}) > 0$ as shown in Fig. 14. Results of $\bar{p}^{\uparrow} p \rightarrow \pi^{\pm} X$ measurements will be available soon.

d) A Short Summary of x_T and x_F Dependences

There are two distinct common phenomena observed in the x_T and x_F dependence of the one-spin asymmetries. The asymmetry values are zero or small for both x_T and $x_F <$ 0.3 - 0.4, with a rise from zero to large positive values for x_T and $x_F > 0.3 - 0.4$. It will be interesting to find out if these two phenomena are related. There are several papers in preparation about physics interpretation of these data which should be ready soon.

e) Double-Spin Asymmetry in π° Production by 200-GeV Polarized Protons and Antiprotons

We report a first measurement of the two-spin parameter A_{LL} for inclusive π° production by longitudinally-polarized protons and antiprotons on a longitudinally-polarized proton target. The hadron asymmetry A_{LL} is defined as the relative difference between the cross sections for beam and target hadrons of equal or opposite helicities,

$$A_{LL} = (\sigma_{\Leftrightarrow} - \sigma_{\Rightarrow})/ \sigma_{\Leftrightarrow} + \sigma_{\Rightarrow}) = P_B^{-1} \bullet \langle P_T \rangle^{-1} \bullet (N_{\Leftrightarrow} - N_{\Rightarrow})/(N_{\Leftrightarrow} + N_{\Rightarrow}),$$

where $\sigma(s, x_F, p_T)$ are the invariant cross sections for inclusive π° production in antiparallel ($\Leftrightarrow$) and parallel ($\Rightarrow$) spin states of the beam and target particles. Since the incident hadrons have opposite momenta in the c.m. of the interaction, the helicities are equal when the spin directions are antiparallel. The quantities $N(s, x_F, p_T)$ are the corresponding normalized event rates measured in the experiment, P_B is the beam polarization, and $\langle P_T \rangle$ is the target polarization averaged over polarized and unpolarized nucleons.

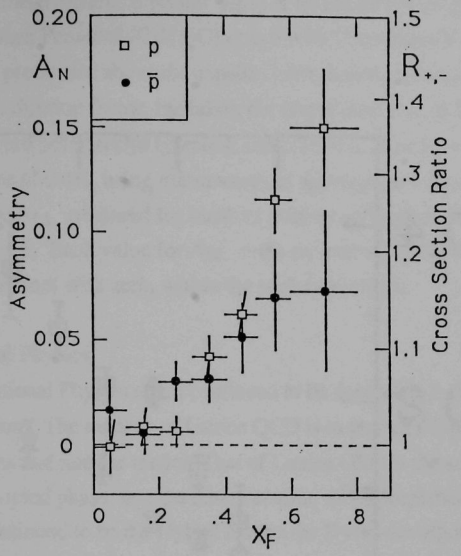

Fig 12. x_F dependence of A_N at p_T = 0.5 to 2.0 GeV/c in $p\uparrow p$ and $\bar{p}\uparrow p$ reactions.

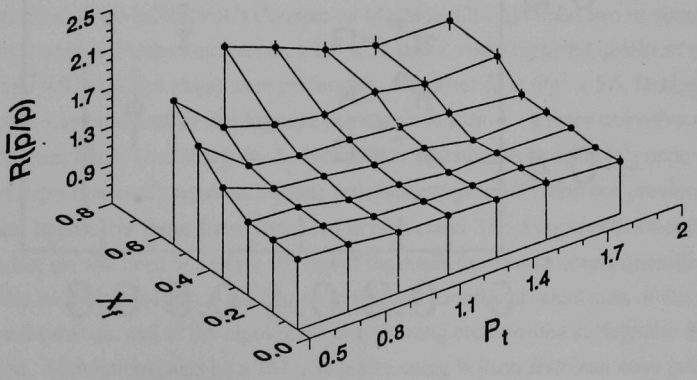

Fig. 13. The ratio $R(\bar{p}/p)$ of the cross section for π° production by antiprotons and by protons.

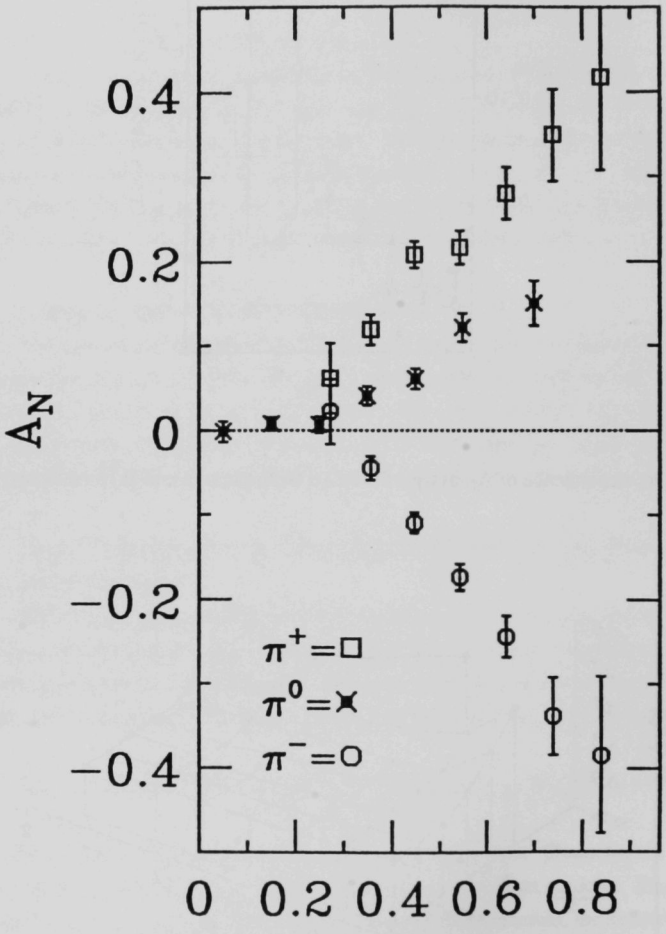

Fig.14. x_F dependence of π° and $\pi^\pm$ production.

The 3-cm diameter polarized proton target of length 20 cm consists of 2-mm diameter beads of frozen Pentanol ($C_5H_{12}O$) doped with Chromium-V. Pentanol contains one polarizable, free proton for about six unpolarizable, bound protons and neutrons. The effective polarization-dilution factor, including the target windows, is $D = P_T/\langle P_T \rangle = (8 \pm 1)$. The free protons are polarized to typically either $P_T = 0.75$ or $P_T = -0.80$ in 3 to 4 hours at a temperature of 0.4K, using microwaves of appropriate frequencies near 70 GHz.

The results for A_{LL} measured for incident protons and antiprotons as a function of p_T, are shown in Fig. 15. Each value for A_{LL} in the p_T interval covered by these measurements is consistent with zero, within the statistical errors.

5. Computational Physics

The Computational Physics effort continued to be devoted to Lattice QCD and Lattice QED simulations. The mission of Lattice QCD is to predict the properties and interactions of hadrons and nuclear matter. That of Lattice QED is the search for the proposed strongly coupled phase, and the determination of its properties. Simulation methods of choice continued to be the Hybrid Molecular Dynamics algorithm for Lattice QCD or QED with dynamical "staggered" fermions, and the related Hybrid Monte Carlo method for Wilson fermions. For quenched QCD we used the Metropolis Monte Carlo method combined with the Overrelaxation method.

Our zero temperature lattice QCD studies aimed at determining low lying hadron (including glueball) masses and other matrix elements have been performed as a part of the multi-institutional HEMCGC collaboration which uses a DOE "Grand Challenge" grant of computer time on the SCRI (FSU) Connection Machine (CM-2) to perform its simulations and measurements. Production runs on a $16^3 \times 32$ lattice with staggered quarks of masses of 0.01 and 0.025 (lattice units) were performed on this lattice at $6/g^2 = 5.6$. During this period code was produced by the Argonne contingent to measure a more extensive set of states than previously (including the Δ. Preliminary measurements using this code on a subset of these new configurations indicate satisfactory agreement with our previous runs on smaller lattices, for those states measured in both cases. The Δ appears heavier than the nucleon, but we will need to analyze the rest of the configurations to obtain quantitative results. We have also started measurements aimed at a variational calculation of the glueball masses and mixings, and of the topological charge using code written at Argonne during this period. Simulations, also on a $16^3 \times 32$ lattice using Wilson fermions were performed at $6/g^2 = 5.3$ for various hopping parameters so that we can compare the two fermion methods.

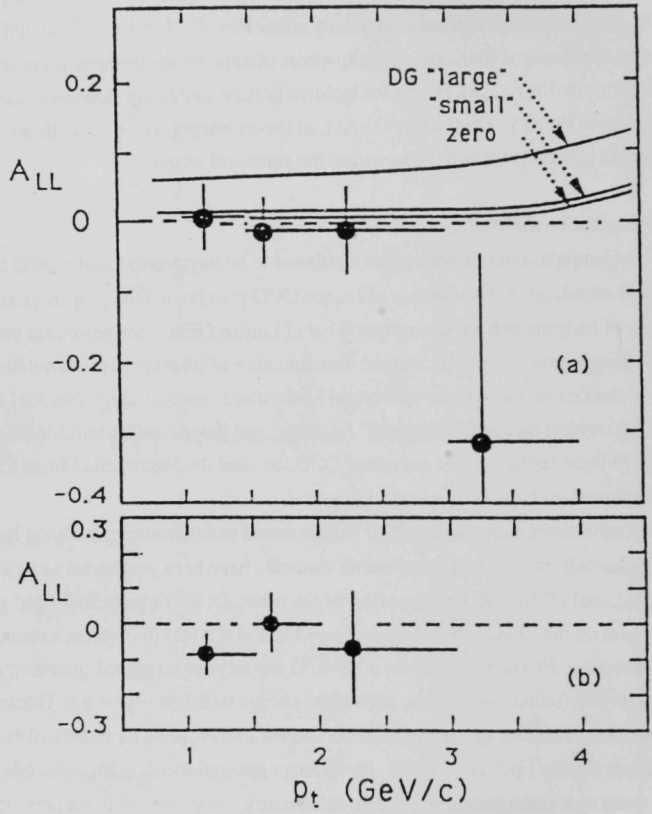

Fig.15. The two-spin parameter A_{LL} in the reaction (a) $p^{\uparrow}p^{\uparrow} \rightarrow \pi^{\circ}X$ and (b) $\bar{p}^{\uparrow}p^{\uparrow} \rightarrow \pi^{\circ}X$ at 200 GeV, for $-0.1 < x_F < 0.1$. The curves are predictions for different values of the spin-weighted gluon distribution function.

As part of a new collaboration formed last year from members of the HEMCGC we have been studying two flavour QCD thermodynamics on a 16^3 x 8 lattice at a quark mass of 0.0125 on the CM-2 at PSC (Pittsburgh). Here we have found that the transition from nuclear matter to a quark-gluon plasma occurs at $6/g^2 = 5.5125 \pm 0.025$. The "time" development of the order parameters near this transition show large fluctuations on many time scales (Fig. 16). This suggests the existence of a nearby critical point rather than the first order transition that appears to exist for > 2 light flavours. We are measuring the energy densities and hadron screening lengths as well as the chiral order parameter $\overline{\psi}\psi$ to try to better understand what observable changes occur in nuclear matter at this transition so that it might be recognized if it occurs, as expected, in relativistic heavy ion collisions.

We have been preparing to perform quenched QCD spectrum calculations using the Current Supercomputing Consortium's Intel Touchstone Delta computer. These will be performed on a 32^3 x 64 lattice with $6.0 \leq 6/g^2 \leq 6.5$ using Metropolis Monte Carlo and Overrelaxation simulations. This will enable us to measure hadron spectra with much smaller quark masses than have been possible before using the conjugate gradient algorithm to obtain the quark propagators. We have produced and tested a Monte Carlo VAX program structured so as to make conversion to the parallel Delta relatively straight forward, as well as a similarly structured conjugate gradient routine

Our work with J.B.Kogut and R.L.Renken of the University of Illinois, S.Hands of the University of Glasgow and A.Kocic of the University of Arizona, on Lattice QED is nearing completion. Preliminary results of our simulations on 16^4 lattices using the CM-2's at NCSA (University of Illinois) and NPAC (University of Syracuse) indicate that, as suggested by simulations on smaller lattices on CRAY's at SCRI and NERSC (Livermore), the transitions observed by several groups in this system are driven by lattice artifacts, and are not indicators of continuum physics. One of us (K. Wang) is now looking at 3 dimensional lattice QED with J.B.Kogut. This is believed to have relevance to high T_c superconductivity.

During this period the Teraflop consortium, of which I am a member and whose goal is to acquire a computer with performance capabilities in the Teraflop range for Lattice Gauge Theory, submitted a second preliminary proposal. More recently we have made modifications of this proposal and expect to submit an official proposal in July.

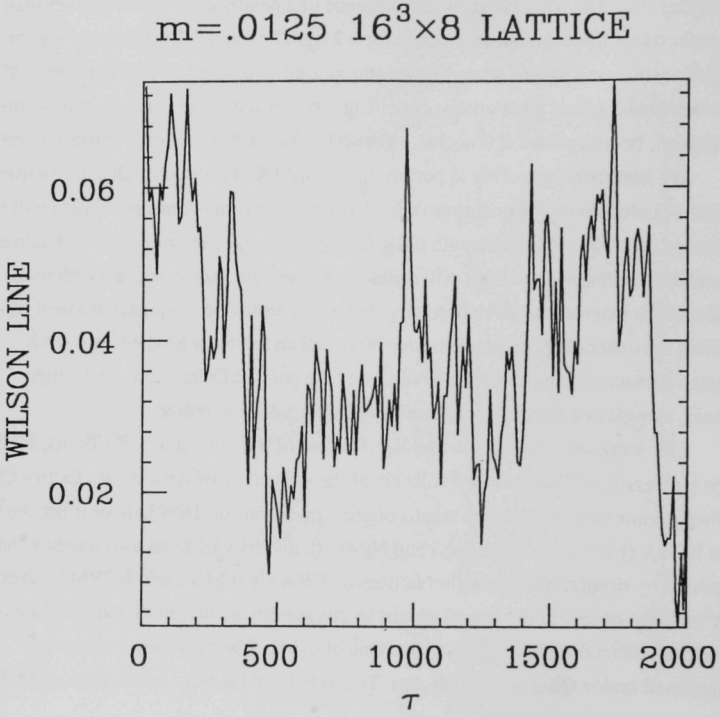

Fig. 16. Wilson Line time evolution at $6/g^2 = 5.525$

B. Experiments Taking Data

1. Soudan 2

The Soudan 2 experiment recorded data for 145 days of livetime during the first half of 1991, with a record high duty cycle of 80%. This brings the total exposure to 695 days, or 63% of a fiducial kiloton year for contained events. The detector is operated for physics data primarily during night and weekend periods when installation work is not in progress and the underground laboratory is unoccupied. Figure 17 shows the number of reconstructed cosmic-ray muon tracks recorded per week of Soudan 2 operation since the beginning of January 1989. The effect of the gradually increasing detector mass over the two year period is evident.

The quality of the data recorded by Soudan 2 continued to improve during the first half of 1991. As described below, the detector mass was increased by about 70 tons during this period, and many of the cracks between active shield floor panels were filled as 170 new shield tubes were brought into operation. New diagnostic software allowed the identification and repair of malfunctioning channels in both the main detector and the shield. The response uniformity of the main detector also continued to improve as the installation of anode high voltage splitters and the fine tuning of anode high voltages continued.

An important milestone was reached in June with the initial operation of the new cosmic-ray air-shower surface array, which now operates in coincidence with Soudan 2. The first surface-underground coincidences were observed at the expected rate of about 75,000 per year. The surface array consists of a 40 m^2 array of proportional tubes to detect electrons from the air showers which produce multiple muon events in Soudan 2. The geometry is shown schematically in Fig. 18. Triggers from the underground detector cause data from the surface array to be transferred to the underground data acquisition computer. Performance and reliability of the surface array will improve as minor technical problems are solved and better diagnostic software is brought into operation. (D. Ayres)

2. Medium Energy Spin Physics

In the past several years, the goal of the ANL-HEP medium energy physics program has been to measure sufficient np elastic scattering spin observables in order to determine the I = 0 amplitudes or phase shifts between kinetic energies of ~ 500-800 MeV. The measurements were performed at Los Alamos (LAMPF) in experiments E-665/770, E-960, E-876, and others.

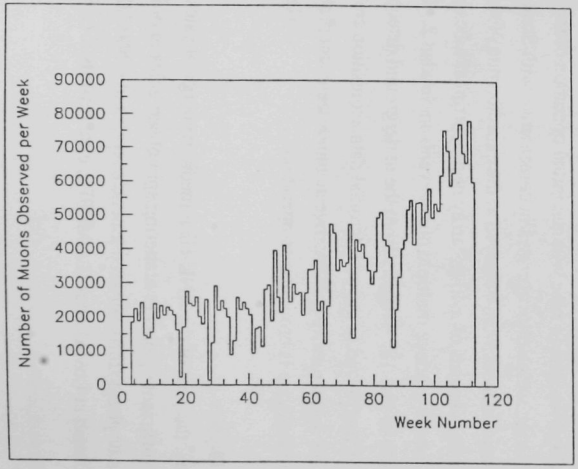

Fig. 17. The number of reconstructed muon tracks per week recorded in the Soudan 2 detector. Week 1 is the week beginning January 1, 1989. The increase in the detector size over the two year period is evident.

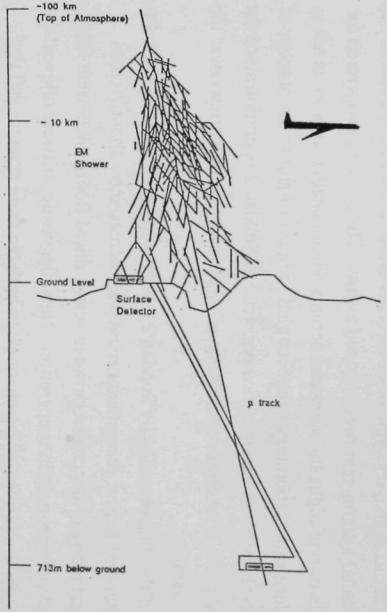

Fig.18. Schematic representation of the surface-underground coincidence experiment which has just begun data acquisition at Soudan. Only the highest energy air showers reach the earth's surface to count in the surface array. Only showers which produce more than one muon in the underground Soudan 2 detector are useful in the study of primary cosmic-ray nuclear composition. About 15% of the 75,000 surface-underground coincidence events per year have multiple muons in Soudan 2.

The data analysis from experiment E-665/770 has progressed substantially during the past six months. This experiment had a polarized neutron beam incident on a polarized proton target, with the outgoing proton detected in a magnetic spectrometer. Essentially final values for C_{LL} and C_{SL} between 80° - 180° c.m. at 484, 634, and 788 MeV, and for C_{SS} and C_{LS} between 30° - 80° c.m. at 484, 634, 720, and 788 MeV have been derived. Small corrections caused by differences in the neutron beam spin direction from the nominal still need to be included. Drafts of two papers on these results have been written and will be submitted in the next period. A third paper from the same experiment, dealing with the np $\rightarrow$ dπ° reaction, is also being written and will be submitted in the next six months.

The total np cross section difference between antiparallel and parallel longitudinal spins ($\Delta\sigma_L$(np)) at 484, 567, 634, 720, and 788 MeV was measured in E-960. A paper on E-960 was recently published in Physics Letters, and an instrument article on the neutron counters used in the experiment was submitted to Nuclear Instruments and Methods. An ANL and a New Mexico State University physicist have worked on a major paper on E-960, including documentation of the many experimental tests, estimates of possible systematic errors, and physics interpretations. This major paper is expected to be completed in the next few months.

Experiment E-876 measured np elastic scattering of a polarized neutron beam, from the new high-intensity optically pumped polarized ion source, incident on a liquid hydrogen target. The momentum of the outgoing proton was measured in a magnetic spectrometer, and the proton spin determined in a carbon polarimeter. The outgoing neutron was detected in coincidence in the same neutron counter array used for E-960. A paper describing the 1990 data at 788 MeV is ready for submission to Physical Review. Preparations for runs in 1991 at 634 and 720 MeV are in progress, but data collection has been delayed by concerns for possible radiation problems if two magnets in the LAMPF beamlines fail simultaneously.

A new DOE funding proposal for future work at Saclay Laboratory in France was submitted before the end of 1990. This proposal was approved in February, 1991, and construction work began on two multiwire proportional chambers (MWPC's). The experimental program goals will be 1) the determination of the I = 0 nucleon-nucleon amplitudes from pn quasielastic scattering of deuterium between 1100 - 2700 MeV, and 2) a clarification of the cause of energy dependent structure near 2100 MeV. ANL contributions to the program will include two new MWPC's and associated electronics, assistance with a new data acquisition system based on a SUN workstation, and manpower for data-taking, analysis and paper writing. The experimental program was recently

approved by the Saclay "Comite des Experiences" (PAC), and a first run is planned for the Fall of 1991. It is hoped to have one of the MWPC's installed and read into the data acquisition computer by the beginning of the run. The second MWPC will be a chamber used in Fermilab E-704, modified for the requirements of the Saclay experiments, and will be completed by the end of 1991. (H. Spinka)

C. Experiments in Preparation Phase

1. Collider Detector at Fermilab

Assembly of preradiator chamber is nearing completion. Of the 95 (plus spares) chambers required, 89 have been completed and tested. Three arches (72 chambers) have been installed and the program of *in situ* testing is continuing. Completion of assembly will allow emphasis on *in situ* checkout of preradiator, crack and strip chambers in preparing for the next run.

The current Fermilab running schedule involves a fixed target run which is just beginning and is scheduled to end in November to allow linac upgrade construction. Collider running should begin early 1992 and last for about two years, interrupted by a 3 - 6 month shutdown for linac upgrade installation. Integrated luminosity goals for before and after have been given by the lab as 25 and 75 pb^{-1}. After a fixed target run, collider operation would resume with the new bunch timing.

The CDF upgrade proposal has been reviewed by the PAC and a technical panel. The only reservation, other than "subject to the availability of funding" was the need for a single muon trigger in the toroids. Fermilab management anticipates that eventually the physics emphasis of the collider program will change from searches (top, etc.) to detailed measurements of bottom. The collaboration has begun to explore possibilities for the evolution of CDF along those lines.

A preliminary design for a Level 2 strip chamber preradiator electron trigger has been made. Further study has confirmed its cost, effectiveness, and viability (see Fig. 19). Our group will take particular responsibility for electronics upstairs for receiving and sifting the signals. Detailed design is proceeding with the goal of partial installation this winter and complete availability by the linac upgrade installation.

The SDC tile measurement work has implied some level of involvement in the CDF end plug upgrade effort.(see Section V.B.4) (L. Nodulman)

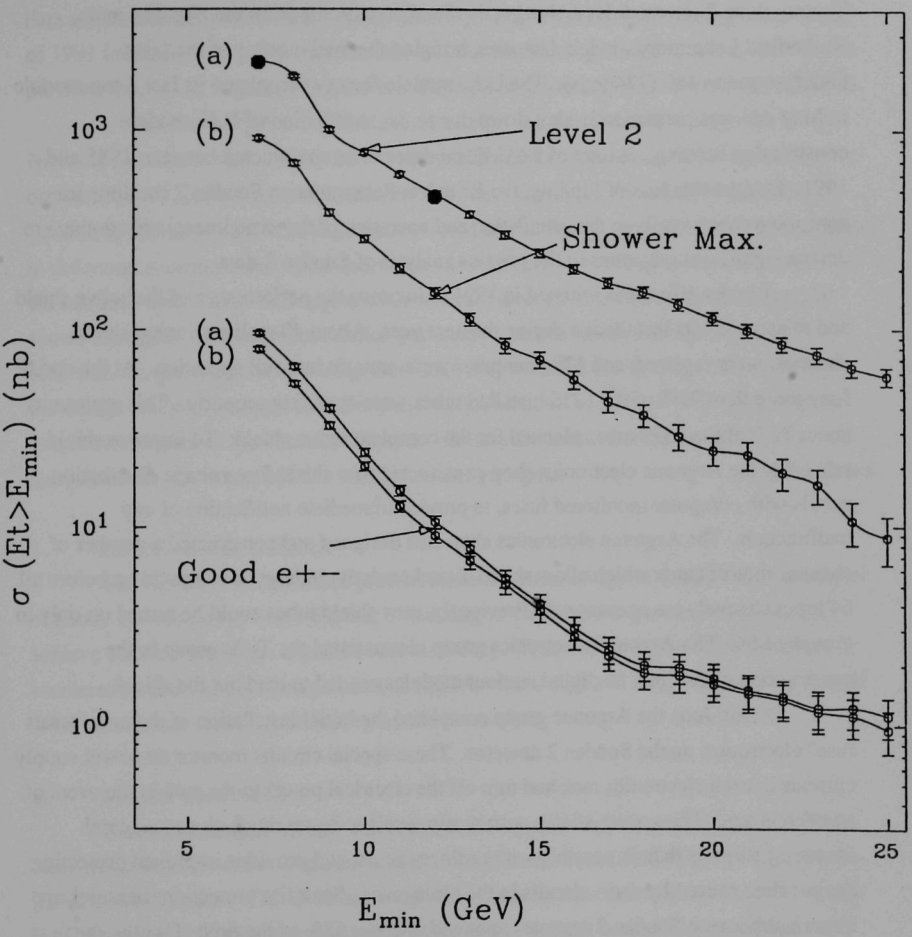

Fig 19. Cross sections for electrons at the Level 2 trigger and after offline selection for (a) Level 2 as run and (b) Level 2 with shower maximum requirement. The black dots are the levels as used.

2. Soudan Detector Installation

Two new halfwalls were added to the Soudan 2 detector during the first half of 1991, bringing the operating mass to 688 tons and the fiducial mass to 541 tons. (A halfwall is a subassembly of eight 5-ton modules, stacked four across and two high.) Twenty three 5-ton modules arrived at the Soudan mine site from the Argonne and Rutherford Laboratory module factories, bringing the total number of modules underground to 180 (774 tons). The U.K. module factory completed its last 5-ton module in May and was permanently shut down due to the termination of U.K. module construction funding. A total of 72 U.K. modules were constructed between 1985 and 1991. Despite this loss of funding, the British collaborators on Soudan 2 continue to contribute substantially to the installation and operation of the experiment, and continue to devote significant resources to the physics analysis of Soudan 2 data.

A major effort was initiated in 1991 to improve the performance of the active shield and to complete its installation during the next year. About 40 malfunctioning shield channels were repaired, and 170 new tubes were brought into full operation. At the end of June more than 99% of the 1216 installed tubes were operating properly. This represents about 77% of the 1572 tubes planned for the complete active shield. To improve shield reliability the Argonne electronics shop constructed new shield low voltage distribution panels with computer monitored fuses, to provide immediate notification of any malfunction. The Argonne electronics shop also designed and constructed a number of channel shutoff cards which allow shield digital readout modules to be turned on before all 64 input channels are operational. Previously, new shield tubes could be turned on only in groups of 64. The Argonne electronics group also assisted the Tufts group in the construction of the final 16 digital readout modules needed to read out the shield.

During June the Argonne group completed the initial installation of the new "smart fuse" electronics on the Soudan 2 detector. These special circuits monitor dc power supply currents in each electronics rack and turn off the electrical power to the rack in the event of an overcurrent. The system allows current trip levels to be set much closer to actual operating currents than is possible with ordinary fuses, and provides improved protection against fires caused by short circuits in the electronics. Such fire protection measures are important because Soudan 2 operates unattended about 65% of the time. Finally, the Argonne electronics shop began the fabrication of final order of 134 preamplifier assemblies which are needed to instrument the full 1030 ton detector.

In January the assembly of proportional wire readout planes for 5-ton Soudan 2 modules was moved from the Argonne module factory to the Soudan mine site. The epoxy potting operation for high-voltage splitter hardware was moved from Argonne to Soudan at

the same time. Components of readout planes and splitters continue to be supplied by Argonne. The shift of these labor-intensive assembly operations to Soudan allowed the technician staff level at the Argonne module factory to be reduced by 20%.

Argonne physicists continued to play a major role in the installation, turnon, and data acquisition activities at the Soudan mine site. Important activities during the first half of 1991 included electronics maintenance and troubleshooting, smart fuse installation, gas purification system upgrades, and the coordination of shield and main detector installation.

In March the Soudan 2 collaboration submitted its proposal (P-822) to the Fermi National Accelerator Laboratory for a long baseline experiment to search for neutrino oscillations. A 30 GeV neutrino beam from the new main injector would be aimed at Soudan 2, 800 km away. The experiment would search for the appearance of tau neutrinos in the muon neutrino beam by measuring the neutral current to charged current ratio. Most tau neutrino interactions will appear to be neutral current events in Soudan 2. Figure 20 shows the region of neutrino oscillation parameter space to which the experiment is sensitive. Argonne physicist Maury Goodman is spokesman for the experiment, and led the design study effort within the Soudan 2 collaboration. In April, P-822 was presented to a subcommittee of the Fermilab Physics Advisory Committee at the Fermilab Director's Review of the new main injector conceptual design report. (D. Ayres)

3. ZEUS Detector at HERA

The HERA machine stored protons at the injection energy of 40 GeV with a lifetime of about 60 minutes in May. Further $e^{\pm}$ running to establish the feedback system and achieve the design current is planned for June-July. This will be followed by ramping, acceleration and multibunch operation of HERA, with the Hl and ZEUS detectors expected to be moved into their interaction regions in November.

a) Module Construction

Barrel calorimeter module construction at Argonne was completed in April. The calorimeter consists of two separate sections, the electromagnetic (EMC) and the hadronic (HACl, HAC2) parts. The EMC stacking of 32 modules was finished in February and the HAC stacking of 20 modules in April. A total of 22 modules were fully assembled and tested at Argonne in the two year period from April 1989 to April 1991.

The parallel effort in module construction at the KFA-Julich Laboratory was completed in May. A total of l0 modules were fully assembled at Julich and shipped directly to DESY. A summary of module construction is shown in Fig. 21. The design and construction of the BCAL modules was written up and submitted for publication to

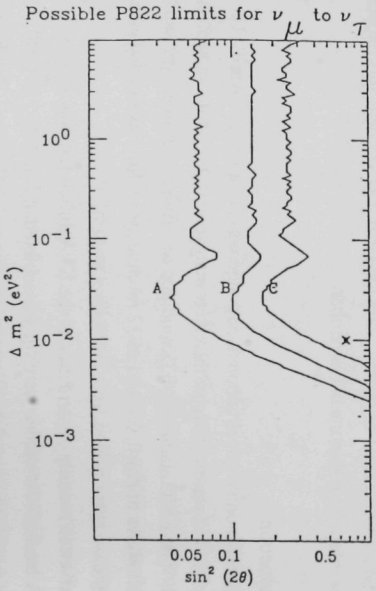

Fig. 20. Regions of neutrino oscillation parameter space which can be excluded by the Fermilab-Soudan long baseline experiment P-822. Regions to the right of the curves are excluded if ν_μ to ν_τ oscillations do not occur. The three curves are for three different measurements of the neutrino flux which can be made with Soudan 2. The point at $\Delta m^2 = 10^{-2}$ eV^2 shows the best-fit oscillation parameters suggested by the Kamiokande atmospheric neutrino measurement.

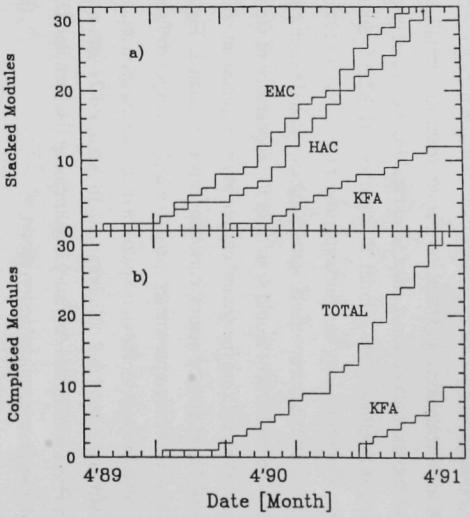

Fig. 21. History of ZEUS BCAL module production:
(a) Number of stacked sections versus time,
(b) Number of completed modules versus time.

Nuclear Instruments and Methods. Completion of the construction of the 32 modules occurred some two months later than originally scheduled in March 1989.

b) Module Testing

All 22 of the modules assembled at Argonne were tested in the cosmic ray facility. Modules were compared quantitatively in terms of (a) the mean charge from a minimum ionizing particle (MIP), (b) the photoelectron yield from a MIP and (c) the attenuation length of the scintillator in a tower (HACl, HAC2 or EMC). After correction for small systematic effects in the electronic readout, it was concluded that systematic module to module variations for the HACl and HAC2 towers were smaller than l%, as shown in Fig. 22 for the HACl towers. For the EMC towers these variations were less than 2%, as seen in Fig. 23.

For the modules assembled at Julich it was not possible to perform cosmic ray quality assurance tests. However, a simple test station was used which allowed the photomultiplier (PMT) high voltage to be set and the current resulting from the uranium activity to be read out. Since it is possible to estimate the MIP photoelectron yield from this information, knowing the PMT gain, some limited comparison with modules assembled at Argonne was possible. This comparison is shown in Fig. 24 for side A of the modules and the agreement is quite satisfactory. The agreement for side B is similar.

Operation of the ZEUS test beam facility at FNAL began in June. In June and early July, a total of three production modules and the prototype will be mapped in detail using muons with the single module mounted on the muon stand. It is anticipated that all four modules will be loaded onto the theta-phi stand in late July and the detailed response of each production module to electrons, muons and pions will be studied before the modules are moved to Argonne on our about August l0 to be prepared for shipment to DESY late in August.

c) Module Shipping

Module shipping from both Argonne and Julich to DESY was accomplished using four 20 foot ocean going containers outfitted with a transportation fixture constructed at Argonne. A total of 29 modules were shipped to DESY with the last one arriving May 23 from Julich. Three modules will remain at Fermilab to undergo detailed testing at the ZEUS test beam facility established in Lab E. No significant module damage was observed in carrying out these complex maneuvers.

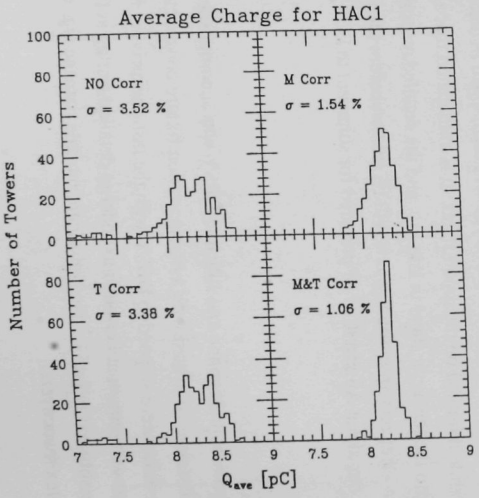

Fig. 22. Spectra of mean MIP charge for all HACl towers tested: (a) without correction, (b) with module-to-module variations due to readout electronics variation removed (22 constants), (c) with the common tower-to-tower variations removed (l4 constants) and, (d) with both corrections (36 constants).

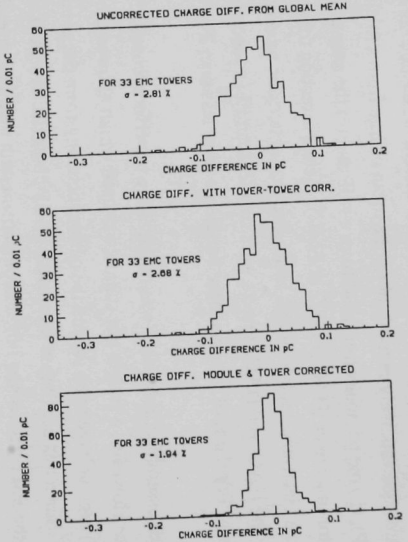

Fig. 23. Spectra of mean MIP charge for EMC towers (33) (a) without correction, (b) with module to module variations removed (l6 constants) and (b) with both module-to-module and common tower-to-tower correction (49 constants).

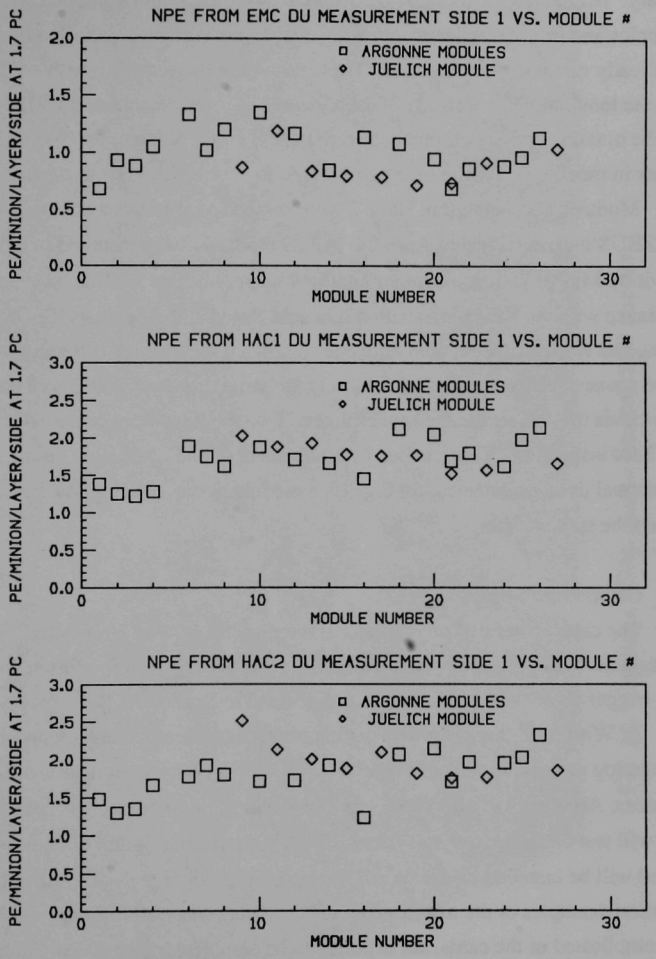

Fig. 24. The mean MIP photoelectron yield side A of the EMC, HACl and HAC2 sections of modules assembled at Argonne and at KFA-Julich.

d) Module Checkout and Installation in ZEUS

A module checkout facility was established at Halle 2 at DESY during January and February. All modules arriving at DESY were modified and/or equipped with their analog electronics and HV controller, as necessary. They were then subjected to many of the same tests already carried out at Argonne. These tests included scanning with a ^{60}Co source to check the longitudinal uniformity of each tower and measurement of the MIP light yield from the uranium activity current and from laser light pulse injection. No significant changes in module performance were observed to have resulted from the transportation.

Modules checked out in Halle 2 were shipped over to the south HERA hall, which is the ZEUS location, starting April 24. All 29 modules, were installed in the ZEUS detector by May 31 with some minor additional work on June 3. This installation was in compliance with the ZEUS installation schedule issued at the February ZEUS collaboration meeting and was carried out with only one significant incident. A differential rotation of the two spokesplates occurred and at closely the same time two modules came into contact with a clevis used to secure the spokesplates. Two modules were removed and returned to Halle 2 for inspection. This resulted in replacement of one EMC light guide with otherwise no structural damage detected. In Fig. 25, a module is shown being lowered into place between the spokesplates.

e) Calorimeter Trigger

The calorimeter first level trigger is the responsibility of University if Wisconsin and Argonne. The trigger processor, which digests the trigger information and decides which trigger algorithms are satisfied, is discussed in Section III.B.

At Wisconsin there is now a working trigger test setup which incorporates the Nevis analog electronics and will be used to check out component boards of the trigger. In September, Argonne will provide an input card and a communications card to the setup, which will test the entire trigger system. The trigger sum cards and fanouts will be ready in July and will be installed on the BCAL modules in ZEUS in early August. The first production examples of the trigger encoder cards were received in June and all of these, the most complicated of the cards, are expected to be complete by the end of August. The adder cards are late because of a redesign to separate some of the functions to a second card; the layout was completed in June. The SDC card is expected to be completed by early July. The first level calorimeter trigger is now a critical path item for the systems integration test in September.

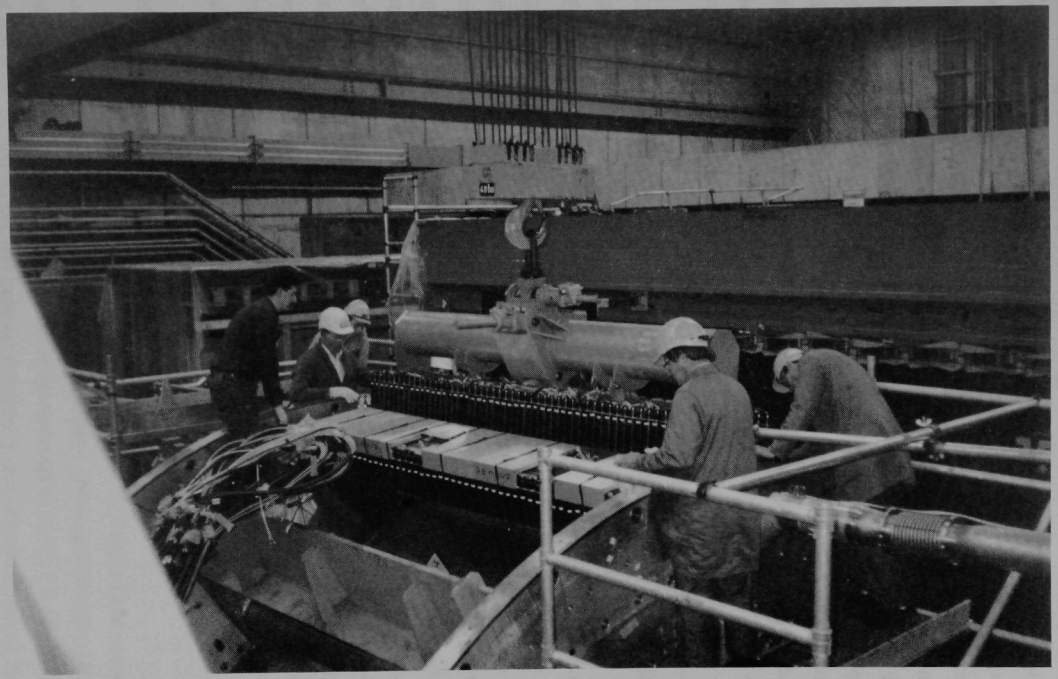

Fig. 25. Loading a BCAL module into the ZEUS detector.

f) Projected Activities for July - December

The installation of services in the rucksack will continue in July. Cabling of the BCAL together with installation of the cooling water manifolds for the analog electronics will be completed in July. The power supplies for the analog electronics and PMT high voltage are expected to become available in August. Until that time only limited checkout of the installed modules will be possible. The magnetic field will be turned on at the end of August and measurements of magnetic forces will be made for the final configuration. A systems integration test will take place in September with a limited cosmic ray test of some detector components. The last three BCAL modules are expected to be installed in early in October and the detector completed, closed up and moved into the beam in the November-December period. The goal is to observe e-p interactions early in 1992. (B. Musgrave)

II. THEORETICAL PROGRAM

Theorists in the High Energy Physics Division have pursued a wide range of topics covering both the formal and phenomenological aspects of particle theory.

Heavy Flavor Production at Collider Energies

E. Berger and R. Meng have continued their studies of the hadroproduction of heavy quarks at collider energies. In a recent paper (ANL-HEP-PR-91-34) they provide predictions of the distribution in the transverse momentum of the quark/antiquark pair. Just as in massive lepton pair production, lowest order QCD leads to the expectation that the quark/antiquark pair will be produced with very little transverse momentum. Next-to-leading order contributions generate transverse momentum through gluon recoil. However, the prediction at next to leading order is not reliable at relatively small values of p_T of the pair, where the cross section is largest, in spite of the fact that a large momentum scale is present, viz., the invariant mass of the heavy flavor pair. This situation is an example of the problem of calculating a cross section in perturbation theory when two different momentum scales are present. The perturbation series in such cases involves logarithms of the ratio of the scales. When one of the scales becomes much smaller than the other, the logarithm may become of order unity, and the perturbation series must be treated by alternative methods. To deal with this problem, Meng and Berger have employed soft gluon resummation techniques. Among other results, they calculate that the average value of p_T of the bottom/antibottom pair is in the range of 6 to 7 GeV at $\sqrt{s} = 1.8$ TeV. Since the typical value of p_T of a single b (or anti-b) quark is about 5 GeV at the same energy, Berger and Meng predict a significant imbalance in the transverse momenta of the bottom and antibottom quarks. In addition to their interest for further tests of perturbative QCD, the results have important implications for plans being developed to search for CP noninvariance in the B system at hadron colliders.

Prompt Photon Production

J. Qiu (State Univ. of N.Y., Stony Brook) and E. Berger have continued their studies of the theory and phenomenology of prompt photon production at hadron collider energies. Their solution to the photon isolation problem (ANL-PR-90-104), discussed in the last semi-annual report, has been accepted for publication in Physical Review D. Berger and Qiu are now working to translate their analysis into a practical numerical program that can be made available to experimenters. The program will allow users to calculate both the fully inclusive and the isolated prompt photon cross section at various

energies, values of transverse momentum p_T, and choices of the isolation parameters. Their calculations are done at next-to-leading order in perturbative QCD and include a careful treatment of the contributions from the non-perturbative, long distance quark and gluon fragmentation terms. The fragmentation terms account for about half of the inclusive cross section at small x at collider energies.

Perturbative QCD Explanation of "Massive" Sea Quark Distributions

In a recent paper (ANL-HEP-PR-91-50), R. Meng has presented a QCD parton model in which the non-perturbative intrinsic components of the "massive" sea quark distributions are assumed to be very small. The perturbative components of the "massive" sea quark distributions can be approximately determined in terms of $F_2^{\gamma^* g \to q\bar{q}}$ by perturbative QCD. In fact they can be computed using the QCD running coupling constant, the measured gluon distributions and the current quark masses m_q determined by chiral symmetry breaking. In this model the flavor SU(3) symmetry for the sea quark distributions is explicitly broken due to the different current quark masses. The prediction on the relative sizes of the perturbative sea quark distributions $b_{sea}, c_{sea}, s_{sea}$ is given in terms of simple logarithmic functions of Q / m_q. It is found that the perturbative calculations agree with the up and down sea quark distributions from HMRS parton distributions. This interpretation of sea quark distributions would heavily impact the future global analysis of the parton distributions. It could also make it much easier to pin down the gluon distribution even at small-x region. In addition, the model predicts that the current quark masses can be determined by measuring the massive sea quark distributions accurately. Finally, an accurate measurement of the strange sea quark distribution is urged to test the model and the accuracy of the perturbative calculation.

Transverse Momentum of Higgs Bosons in Gluon Fusion

R. Kauffman's work on the transverse momentum distribution of Higgs bosons in gluon fusion has been prepared for publication (ANL-HEP-PR-91-21, to appear in Phys. Rev. D).

The Odderon, a New Threshold and Confinement

In a paper (ANL-HEP-PR-91-32) to be published in Physics Letters B, A. White and K. Kang (Brown University) have shown that a dispersion relation model with a localized threshold at $\sqrt{s}$ ~ 500 GeV remains compatible with all forward elastic scattering data. This model provides an explicit alternative to the Odderon explanation of the large UA4 real part. Indeed, given the low Tevatron collider cross-section now obtained by both E710

and CDF, and the preliminary real part obtained by E710, this form of threshold is generally thought to be the only way that the UA4 result can be compatible with all other elastic data. The paper also discusses the presence of an Odderon at large transverse momentum in perturbative QCD, and argues that at low transverse momentum confinement is in conflict with the presence of an Odderon. The result of White's general analysis that there is an Odderon in SU(N) gauge theory for $N \geq 4$ is alsonoted.

Asymptotic Amplitude Analysis

A. White and M. Block (Northwestern) have made an asymptotic analytic amplitude analysis of the $t = 0$ parameters for pp and pp collisions in the energy region $\sqrt{s} = 5 - 1800$.GeV. The results are presented in ANL-HEP-PR-91-38 and the conclusions are that 1) a $\log^2 s$ dependence, with or without maximal Odderons, does not fit the cross-section data, 2) a $\log^2 s$ dependence fits the cross-section data, but not the UA4 ρ-value. A maximal Odderon does not improve the fit. The analysis therefore does not lend support to the hypothesis of an asymptotically maximal Odderon. The paper also discusses why the energy region available may simply be too low to be in "asymptopia".

Light Quarks and the Pomeron in QCD

In a paper (ANL-HEP-CP-91-54) presented at the Fourth Blois Workshop on Elastic and Diffractive Scattering A. White has argued that light quarks are essential for the occurrence in QCD of a low transverse momentum Pomeron compatible with confinement and other well-established physical properties. The analysis is based on the contribution of massless quark loops to the interactions of reggeized gluons and the resulting confinement produced by the exponentiation of infra-red divergences. Fundamental features of the argument are the conflict of the necessary transverse momentum cut-off with Pauli-Villars regularization and the origin of a reggeon condensate in triangle anomaly transverse momentum divergences. The outcome is that SU(2) gauge theory has a high-energy limit closely analogous to the two-dimensional Schwinger model, that is the physical states are pseudoscalar mesons and the S-Matrix is "trivial" in the extreme sense that there is no Pomeron.

Extension of the analysis to higher gauge groups shows that there is an even-signature Pomeron in QCD, an additional "Odderon" trajectory in SU(4) gauge theory and N-2 trajectories in SU(N) gauge theory. Implications of the analysis for QCD with a small number of flavors and for the existence of a higher color quark sector associated with with electroweak symmetry breaking are also discussed.

The Standard Model on the Lattice

Over the last several years, G. Bodwin and E. Kovacs (FNAL) have developed a new method for implementing gauge theories involving chiral fermions on the lattice. The standard electroweak model is, of course, a prominent example of such a theory. The method of Bodwin and Kovacs avoids the fermion-doubling problem by employing Wilson fermions. The Wilson mass term explicitly breaks the chiral symmetry; however, the symmetry is restored, in the continuum limit, through the addition of suitable counterterms. Bodwin and Kovacs have shown, to all orders in perturbation theory, that the required counterterms can be generated either through coupling-constant and mass renormalization or through the introduction of two auxiliary Dirac species. These results were reported at the Lattice 90 Conference in Tallahassee, Florida, and are described in a contribution submitted to the proceedings of that conference (ANL-HEP-CP-90-117). During the last several months, Bodwin and Kovacs have derived an alternative formulation for the auxiliary species that may streamline numerical simulations and provide new insights into the physical interpretation of their approach. A publication describing this work is in preparation.

Linearized Lattice QED

Recently Hands, Kogut, and Sloan proposed an alternative formulation of QED on the lattice that is known as linearized QED. Such an alternative formulation might be of use in distinguishing lattice artifacts from physical effects in numerical simulations of strong-coupling QED. G. Bodwin, E. Kovacs (FNAL), and J. Sloan (Ohio State) have pointed out that linearized QED has a serious shortcoming: although the theory is formally gauge invariant, it generates a large number of renormalization counterterms that would usually be ruled out by the gauge symmetry. Such counterterms arise because the gauge symmetry is implemented nonlocally. This work is described in ANL-HEP-TH-91-35.

Quantum Algebras

C. Zachos and D. Fairlie (Univ. of Durham, U.K.) considered applications of the Multiparameter Quantum Heisenberg Algebras they discovered recently. These are associative structures that generalize oscillators, bosonic or fermionic, and may be thought of as "anyonic interpolates" of the two. Fairlie and Zachos found a family of Hamiltonians which possess simple deformed-commutation relations with these new oscillators, and diagonalized them. These Hamiltonians, whose classical limit provides the solution to higher-order derivative systems, could then serve as exploratory models for q-quantization, i.e. the time-evolution of systems of quantum oscillators with unconventional wave

function symmetries. However, spectrum preservation requires unitarity, which dictates that time not be a mere parameter, in this case. For the time being, this makes a direct connection to a specific system in the laboratory problematic, but solutions are currently being worked on.

Quantum Groups

In a paper to be published in the Journal of Mathematical Physics, S. Vokos interprets the covariant differential calculus on the quantum hyperplane acted on by the multiparameter deformation of $GL(N)$ as a deformed oscillator algebra (Heisenberg algebra). In this work (ANL-HEP-PR-91-07), he constructs the corresponding algebra of the quantum group through the Jordan-Schwinger construction. For $N \geq 3$, he shows that this quantum algebra gives quadratic constraints among the generators. However, for $N = 2$ Vokos elevates this construction to a Hopf algebra. He achieves that by finding simple comultiplication rules for the generators, i.e. the rules of combining representations of the general linear group of 2×2 matrices, whose matrix elements satisfy specific non-trivial, deformation parameter dependent commutation relations. Furthermore, he establishes the equivalence of his approach with the other two covariant deformations that appear in the literature, namely the Woronowicz-type two-parameter deformation of Schirrmacher, Wess, and Zumino, as well as the Drinfeld-Jimbo deformation. Vokos is currently investigating applications of this construction to deformed Hamiltonian mechanics problems.

Anomalous Baryon Number Violation:

P. Arnold and M. Mattis (Los Alamos National Lab) have continued to focus on the controversy of whether the weak interactions necessarily become strong at energies around 10 to 100 TeV. The speculation arose from a low-energy calculation done by Ringwald and Epsinosa using instantons. At high-energy, where the controversy rages as to whether the cross-section can become large, the original calculation is invalid because of the presence of large corrections. One method for summing the large subset of these corrections associated with final state corrections has been proposed by Khoze and Ringwald. There was some controversy because the method, known as the "valley method," does not obviously compute the desired physical cross-section. Early in the year, Arnold and Mattis used more fundamental methods to compute the next-to-leading order corrections to the cross-section at small energy as $E \to 0$. The calculation provided an important diagnostic of the valley method, with which it agreed. Recently, they have

proven the formal equivalence of the valley method and more rigorous methods to all orders in the energy E.

Electroweak Vacuum Instability and Mass Limits on the top and the Higgs

The electroweak vacuum need not be absolutely stable. For certain top and Higgs masses in the minimal standard model, it is instead metastable with a lifetime exceeding the present age of the Universe. The decay of our vacuum may be nucleated at low temperature by quantum tunneling or at high temperature by thermal excitation. In a paper submitted to Physical Review, P. Arnold and S.Vokos show that the requirement that the vacuum survive the high temperatures of the early Universe places the strongest constraints from vacuum stability on the top and Higgs masses in the minimal standard model (Fig. 26). If a single Higgs is found experimentally, these constraints may place an upper bound on the scale of new physics beyond the minimal standard model. In this work (ANL-HEP-PR-91-39), Arnold and Vokos examine temperatures very large compared to the scale of weak symmetry restoration and find much stronger bounds than those suggested by other work. They also present a simple analytic approximation that directly relates the bounds to the running coupling constants of the Weinberg-Salam theory.

Calculations of Bottom Quark Production at Hadron Colliders

D. Kuebel has completed his Ph.D. research (U. of Chicago) under the supervision of E. Berger. The thesis studies Monte Carlo simulations of QCD heavy flavor production processes $\left(p\bar{p} \to Q(\overline{Q})X\right)$ at hadron colliders. ISAJET bottom quark cross sections are compared to the $O\left(\alpha_s^3\right)$ perturbative calculation of Nason, Dawson, and Ellis. These Monte Carlo cross sections are computed from data samples which use different parton distribution functions and physics parameters. Distributions are presented in the heavy quark's transverse momentum and rapidity. Correlations in rapidity and azimuthal angle are computed for the heavy flavor pair. Theory issues which arise are the behavior of the cross section at low and high values of transverse momentum and the treatment of double counting problems in the flavor excitation samples. An important result is that ISAJET overestimates bottom quark production cross sections and K-factors. These findings are relevant for estimates of rates and backgrounds of heavy flavor events.

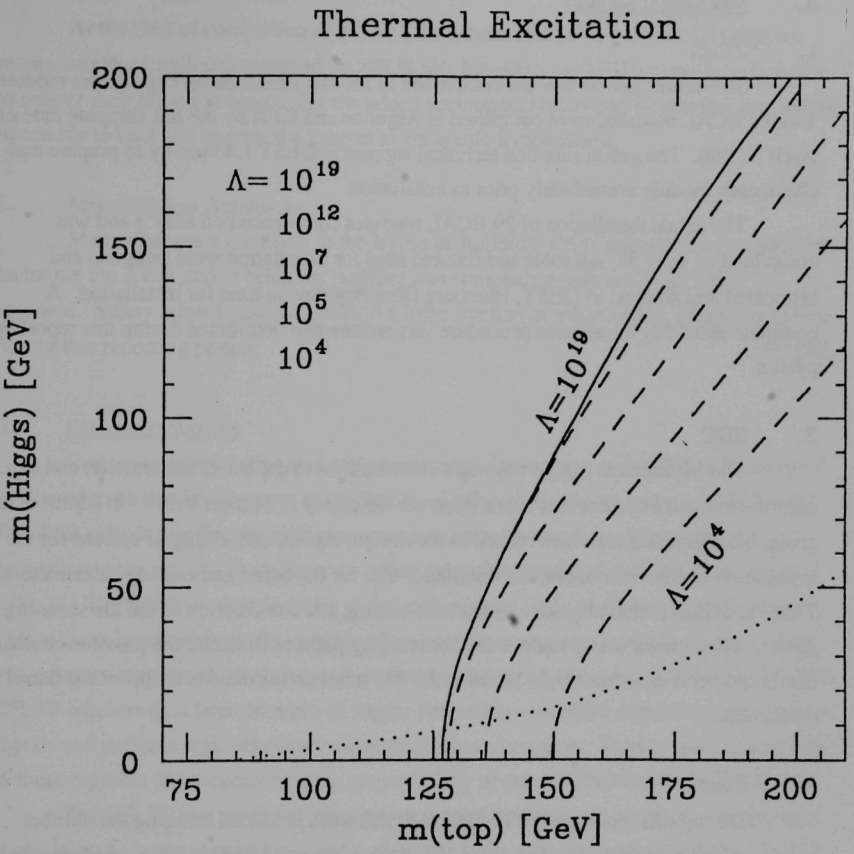

Fig. 26. Results of the Analysis of Arnold and Vokos. For various choices of the scale Λ for new physics beyond the minimal standard model, the region below the corresponding line is excluded because our vacuum would have already decayed by thermal excitation at high temperature. The dotted line is the bound of G. Anderson, from processes below the temperature of symmetry restoration. The total bound is the union of the dotted curve with the appropriate high-temperature curve.

III. EXPERIMENTAL FACILITIES RESEARCH

A. Mechanical Support

1. ZEUS

This report period saw the completion of the last ZEUS barrel calorimeter modules. Twelve BCAL modules were completed at Argonne and KFA by the last shipping date of April 17, 1991. The group supplied technical support at DESY Laboratory to prepare and check each module immediately prior to installation.

The actual installation of 29 BCAL modules commenced on May 3 and was completed on May 31. All tools and fixtures used for installation were designed and fabricated and shipped to DESY, Hamburg from Argonne in time for installation. A complete assembly installation procedure was written and distributed during this reporting period.

2. SDC

The Mechanical Support Group's contributions to the barrel calorimeter, end cap calorimeter, and Fermilab test beam effort are described in Section V.B.3. In addition, the group has supported activities related to the design, layout, and testing of options for the installation of fiber readout on the scintillator tiles for the barrel and end cap calorimeters. These activities included groove design, tile testing, and construction of the tile scanning device. Some work was also done on fiber routing paths to illustrate the possible choices that could be used to route light fibers to the PM tubes on the outside radius of the barrel calorimeter.

3. Soudan 2

During this report period 14 PDK modules were produced bringing the number produced at Argonne to 131. The assembly of the readout wire planes was transferred to the mine in an attempt to reduce overall costs. All components, however, are still being prepared at Argonne by mechanical support personnel.

4. Argonne Wakefield Accelerator

Drawings of the photocathode gun, preaccelerator and associated RF and vacuum equipment were completed during this period. The supports for equipment are being designed this time. Additional designer effort was added to accommodate both the SDC

and AWA projects. (See Fig. 27 for layout of the photocathode gun and front end of the preaccelerator.)

5. MHD

At the time of completion of the ZEUS modules most of the mechanical support manpower that had been employed on ZEUS was loaned to the MHD propulsion program to bolster their efforts in connecting the added vacuum and cryogenic equipment that will be necessary to cool and operate the magnet at cryogenic temperatures.

6. Miscellaneous Activities

Many changes were made to the layout of Building 366 to prepare for new projects, including the AWA and to bring the building into compliance with the Tiger Team response. Safety related issues consumed a large fraction of the available group manpower during this reporting period. (N. Hill)

B. Electronic Support

Our major effort during this period with regard to support of the ZEUS calorimeter continued to be the development of the first-level calorimeter trigger processor (CFLTP). The Zeus calorimeter first-level trigger processor presents summary data on energy deposition in the uranium/scintillator sampling calorimeter to the global first-level trigger (GFLT). The summary data includes global and regional sums of electromagnetic and hadronic energy deposition, the number of isolated muons and isolated electrons, missing transverse energy, jet cluster information, and the likelihood of beam-gas background. The CFLTP receives data from 16 regional trigger pre-processors which digitize the calorimeter signals and perform regional energy sums and logical operations. Design and construction of these regional pre-processors is the responsibility of our collaborators from Wisconsin.

The CFLTP is a pipelined processor that contains data from eight crossing periods at any instant. It can capture input and output data from a sequence of up to 4096 consecutive beam crossings or first-level trigger events for detailed examination. All data variables are accesible for histogramming; the histograms are evaluated by on-board processors that reside in a VME bus, embedded within the the CFLTP. Input or output data emulation capability is provided to operate the CFLTP at full speed in a stand-alone mode. In addition, the design includes a number of utility functions to inspect the data flow and to assist in troubleshooting.

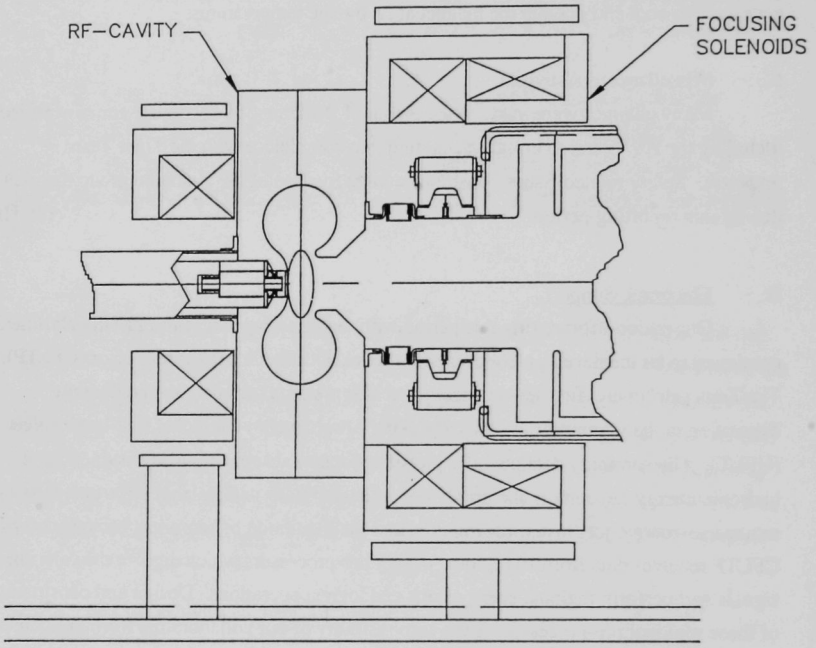

Fig. 27. Layout of the AWA photocathode gun and preaccelerator front end.

During this period our work included:

- Production of a run of four input cards and four output cards
- Completion of the first algorithm card
- Initiation of production on the next 6 algorithm cards
- Initiation of production of the custom backplane
- Production of the cooling system for the custom crate at the detector
- Construction of two large size crates, one for DESY and the other to remain at Argonne
- Continuing design effort on the communication card and the other algorithm cards

In addition work continued to support the nucleon decay experiment, Soudan 2. Our involvment has become one primarily of construction and maintenance. During this period we performed the following tasks:

- Smart Fuse Protections System - Produced 36 systems
- Drift High Voltage Modules - Produced 2
- Shield Voltage Distribution Modules - Produced 4
- HPW Voltage Distribution Module - Produced 1
- Existing Electronics - Maintained as necessary

We are providing support to the MHD Test Facility at Argonne, and during the period designed and produced eight conditioning amplifiers and six CAMAC multiplexers for data acquisition from the thruster. We have become involved in some aspects of the construction of the test facility, and during the period we designed and constructed the shunt rack for monitoring approximately sixty currents to various electrodes in the thruster. We continued support to the physics division by construction of the APEX experiment trigger. (J. Dawson)

IV. ACCELERATOR RESEARCH AND DEVELOPMENT

A. Advanced Accelerator Test Facility (AATF) Program

1. SLAC NLC Cavity Measurements

Experimental activities during this period reflected the group's continuing collaboration with physicists from SLAC on measurements relevant to the design of the Next Linear Collider (NLC), in particular the study of schemes to suppress the multibunch beam breakup instability by damping or detuning parasitic deflecting wakefields in the accelerating cavities. An iris-loaded structure was prepared with a range of iris and cell radii chosen to achieve a Gaussian distribution of HEM_{11} frequencies, resulting in an exponentially decaying envelope of the transverse wake potential. Figure 28 shows the measured transverse wake for this structure. A clear detuning effect is observed, and good agreement between experiment and simulation is obtained when finite bunch length effects are taken into account. Further experiments are under consideration using structures in which HEM_{11} modes are damped as well as detuned, and with measurements extended to very long (3 ns) drive-witness delays.

2. System development

The extremely low intensity of the AATF witness beam requires that a certain amount of processing be applied to the digitized image of the witness beam at the spectrometer focal plane to subtract the background caused by halo electrons from the drive beam. The most successful technique used so far involves fitting the background to a linear function of position in the area of interest (AOI) containing the beam spot and using data from the boundary of the AOI to determine the fit parameters. This method frequently requires operatorb intervention in the selection process, and rapidly fluctuating backgrounds can reduce its effectiveness. A more sophisticated procedure using Fourier transform filtering was examined as a potentially better approach. Raw data consists of 8 bit, two dimensional arrays produced by the CCTV/frame grabber system. A cleaner signal can be produced by performing a 2-D FFT of this data, numerically filtering out high frequency noise, and constructing the inverse FFT. The preliminary results are promising.

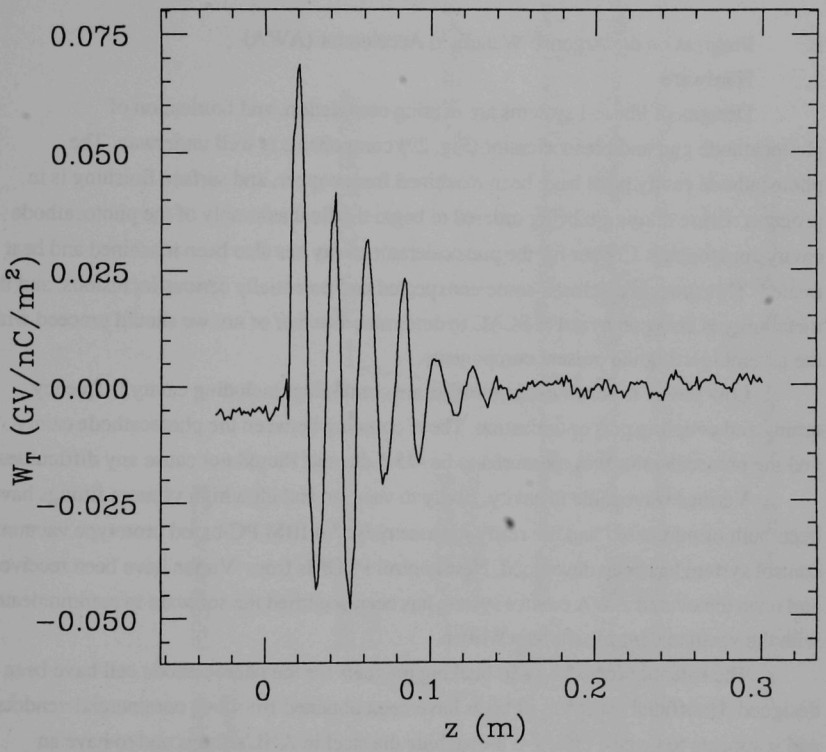

Fig. 28. Measured transverse wake potential for the NLC detuned cavity.

3. Damped structures

In addition to the work being done collaboratively with SLAC, the group has maintained an interest in damped structures of our own design. An iris-loaded version of a deflection-mode-damped accelerator structure is currently being fabricated. Bench tests will be performed in June, and if those tests indicate successful deflection-mode damping, wakefield measurements of the structure will be performed at the AATF this summer.

B. Progress on the Argonne Wakefield Accelerator (AWA)

1. Hardware

Designs of Phase-I systems are nearing completion, and fabrication of photocathode gun and preaccelerator (Fig. 29) components is well underway. The photocathode cavity parts have been machined from copper, and surface finishing is in progress. Braze alloys are being ordered to begin the final assembly of the photocathode cavity components. Copper for the preaccelerator cavity has also been machined and heat treated. This process disclosed some unexpected and potentially serious inclusions, and the metallurgy is being analyzed at SLAC to determine whether or not we should proceed with the assembly using the present components.

Low power rf bench measurements are continuing, including cavity frequency tuning and coupling port optimization. The rf coupling between the photocathode cavity and the preaccelerator was measured to be -45.5 db, and should not cause any difficulties.

Various waveguide to cavity, cavity to vacuum and ultra high vacuum fittings have been built or purchased and are ready for assembly. An IBM PC-based prototype vacuum control system has been developed. New control PROMs from Varian have been received and once the overall AWA control system has been specified the software to communicate with the vacuum control will be rewritten.

The solenoid focussing and bucking magnets for the photocathode cell have been designed. Unofficial estimates of costs have been obtained from two commercial vendors, and it appears to be cost effective to machine the steel in ANL's shops and to have an outside vendor fabricate the coils.

The design of the beam optics for the new wakefield measurement system, which provides a precisely adjustable drive-witness bunch delay, was completed. Many of the components for this system will be recycled from the AATF, and magnets which must be specially built are in various design stages. Work was also initiated on the design of the optics to match the drive and witness beams from the preaccelerator into the wakefield measurement beamlines.

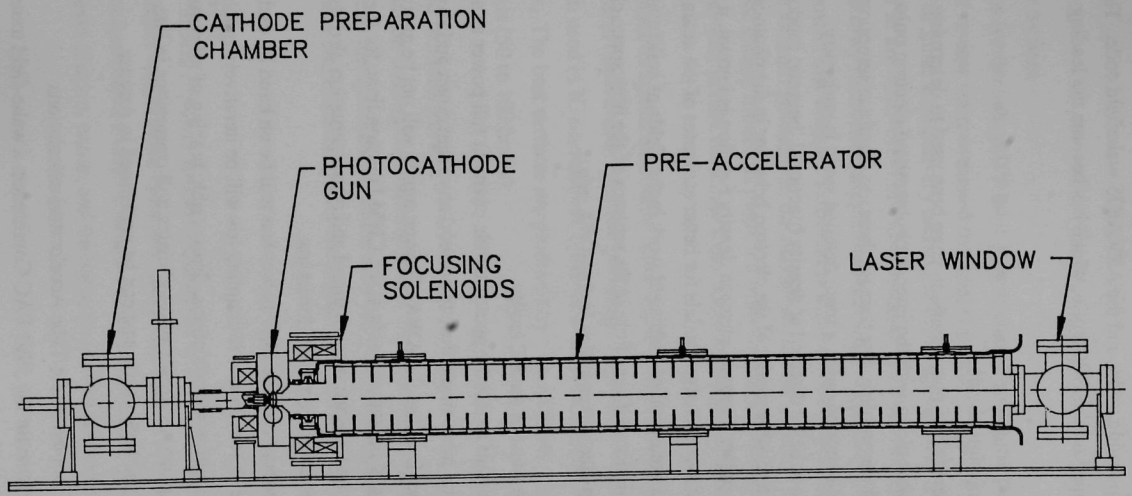

Fig 29. The Argonne Wakefield Accelerator Phase-I linac.

Several workstation options under consideration as control/data aquisition machines for the AWA were benchmarked as to their respective floating point performance using both simple loop timing codes and the ARRAKIS wakefield code. The highest overall speed was obtained on the HP/Apollo, which has become the leading candidate for use at the AWA.

2. Photoemission physics

Simple models of photoemission have been used to determine if large thermionic tails will be present along with the intense photoemitted electron pulse. The work so far indicates little or no problem, but because there are certain assumptions used in these models which may not be valid, a more detailed study is underway.

Research is being directed at density functional theoretic models of solids with the goal of creating a reliable model of the electron behavior in the photocathode upon impact by the UV laser pulse. Once an electron density function is known, it can be coupled to standard cathode space-charge models for better estimates of the actual time response. There has been a great deal of published work in the fields of solid state and of photoelectric emission but very little in the regimes of the high space charge and short time scales relevant to electron emission in the AWA gun.

3. Full power test of the PC cavity

It is important to test the photocathode cavity at full power as soon as possible in order to study (and have ample time to correct) any breakdown and dark current problems which might arise. Because the AWA rf power supply will not be available until summer of 1992, we will use rf power available at the CHM Division linac for these initial tests. Sufficient power and precise power control and instrumentation already exist at the linac and arrangements have been made for its use.

All components for the high-power test will be on hand by end of June. In the first weeks of July the PC cavity and rf coupling iris will be iteratively machined to meet frequency and matching specifications. Irreversible brazing of all parts, assembly of vacuum plumbing, and assembly of diagnostics will commence in late July, and if no major difficulties arise, the high-power test can be performed in August.

4. CWTA (Coupled Wake Tube Accelerator) calculations

As an exercise for the 1991 PAC Conference, a wake-field transformer accelerator (coupled wake tube geometry) was designed to yield an accelerating gradient of 200 MeV/m with drive-to-witness energy conversion efficiency of 10% for the drive beam that

will be available from phase I of the AWA linac. Details of the impedance matching section are not yet determined, but numerical simulation of a reference design has confirmed the CWTA principle.

5. Pulsed Laser System

Specifications for the pulsed UV laser system were submitted to Purchasing in January. A technical review team evaluated the three responses received to an RFQ. A contract was signed in June, with delivery and commissioning expected in early fall, 1991.

Using a laser in the ANL-CHM division, preliminary measurements were made to evaluate the laser intensity fluctuation suppression scheme ("noise eater"). A test assembly was set up which showed that voltages sufficient to drive a Pockels cell were produced from an inexpensive vacuum photodiode, the maximum voltage produced from a photodiode was space charge limited as predicted from Child's law, and that the Pockels cell driven in this way did, in fact, modulate light from a HeNe and UV Excimer laser as expected.

Work continued on spatial smoothing techniques for the laser pulse. After a number of unsuccessful experiments with fire polishing, the etching of ground surfaces with an etch solution used in IC manufacturing seems to be producing surfaces that scatter light at small angles. The best surfaces are produced by fine abrasives (1000 -1200 grade) and long etch periods (50 to 100 hours).

6. Conventional facilities/services

The combination control/laser room structure is presently out for bid. PFS/FPE is providing assistance in the specification and review process. A survey has confirmed that adequate cooling water and electrical power are available in building 366 to easily supply the AWA facility.

7. rf power supply

The main 1.3 GHz rf power supply is finally on order. The procurement and commissioning of this rf supply is the determining item for the AWA schedule, and the procurement process has been a trying experience. Functional block diagrams have been generated for low level rf drive, phase, and timing systems, and fabrication will commence soon.

C. Accelerator Physics

1. Plasma Wake Fields

The electromagnetic modes of plasma-filled dielectric-lined waveguide are being studied in regard to enhanced wake-field gradients over that of non-plasma filled waveguide. Currently, the case in the strong applied magnetic field limit is being analyzed. The general case of an applied magnetic field of arbitrary strength may not offer analytic solutions and would have to be treated with a PIC simulation code.

2. CTRON analysis

An analytical model for the HEM mode damped dielectric wakefield device (CTRON) was developed using parameters close to those of AATF tested devices. The calculated results show reasonable agreement between the model and experiment.

3. Beam break-up instability in dielectric wakefield devices

A gridless particle pushing BBU simulation code was developed to check the validity of earlier estimates. The code calculates the wake potential (including higher order radial modes) generated in the tube by an arbitrary bi-gaussian beam pulse. These wake field are then used iteratively to produce the beam dynamics. External focussing fields are applied to confine the beam and produce an effective "damping" of transverse deflections. For AWA wakefield devices being considered, the new results are consistent with earlier estimates indicating that BBU effects will be controllable in high gradient dielectric wakefield accelerators.

4. Photoproduction of Beauty Quarks

The precise difficulties of Fermilab's Wideband Photon Beam Experiment, E-687, were pinpointed as to why its maximum production of beauty quark pairs is 10^5 per year as opposed to the 10^9 needed for studies of CP violation. The possible advantages of using Compton backscattered laser photons were elucidated.

Preliminary calculations were done which show that it is possible to photoproduce up to 10^8 tau lepton pairs per year using Compton backscattered laser photons. This is slightly more than other proposed tau-charm factories can produce. Also, in the Compton backscattered scheme it is possible to obtain polarized tau leptons, a feature which is unavailable in other schemes.

5. Profile monitor for small beams

Effort has continued on the design of a profile monitor for evaluation at SLAC's FFTB (Final Focus Test Beam). More careful modeling of the energy dependence of the detector efficiency has permitted more useful estimates of limits to the resolution from diffraction. Other effects such as multiple scattering, target ion motion, bremsstrahlung opening angles and the limitations imposed by realistic placement of components on the floor at SLAC have also been evaluated, with the result that the resolution at the SLAC/FFTB and JLC/ATF are about 20 nm. Because this resolution seems to be better than competing systems, a document has been produced that describes the costs and benefits of the method, and this document has been circulated at SLAC for evaluation.

(J. Simpson/P. Schoessow)

V. *SSC DETECTOR RESEARCH AND DEVELOPMENT*

A. Overview of ANL SSC Related R&D Programs

The Solenoidal Detector Collaboration remains the focus of our R&D work for the SSC. The SDC is working to define a baseline design for its technical proposal due in April 1992. Substantial progress is being made on narrowing the range of technical options for several subsystems. In the first six months of 1991, the collaboration has made a concerted effort to estimate the cost of the detector. Argonne and our collaborators at the Westinghouse Science and Technology Center have worked on the detailed cost of calorimetry. It has become clear that the general-purpose detector envisioned by SDC will cost more than the SSC Laboratory has budgeted. A major focus of the collaboration at the end of this reporting period is on ways of reducing the cost of the detector while minimally impacting physics capabilities.

Argonne is working strongly on the baseline design of a calorimeter based on scintillating tile with embedded wavelength shifting fiber to deliver the light to photomultiplier tubes. This approach is grounded in Argonne's past construction of scintillator plate calorimeters for HRS at PEP, CDF at FNAL, and ZEUS at DESY. The requirements of SDC, however, along with new technology and ideas, have produced substantial evolution in design from these examples. Progress on the calorimeter subsystem design is described below.

A few of the Argonne staff are part of the Computing Working Group for SDC, including one of the co-chairs. They organized two workshops during this period: in January at SSCL before a regular collaboration meeting, and in May at Rutgers University. In addition, the working group has met at collaboration meetings in January, March, May, and June. The computing group has made an extensive analysis of requirements for online and offline computing and for several aspects of software and the software development process. An outline has been made of a baseline architecture for costing and iteration. Argonne led a collaboration from within SDC which make a proposal to the DOE Scientific Computing Staff for early start money related to the proposed High Performance Computing and Communication presidential initiative for FY 1992-1996. The subject of the proposal, which received $180K, is a database approach to the major data storage and access problem which SDC will face when it begins taking data. A renewal proposal has also been prepared for FY 1992 and beyond.

The consumers of computing, those doing simulations for the Physics and Detector Performance Working Group are also represented at ANL (including one of the co-chairs). A system of six Silicon Graphics processors has been commissioned for this group. Four

processors are in workstations with screens on individuals' desks. The other two are configured as severs with larger disks. Computations being pursued with this system include $H \rightarrow ZZ \rightarrow \ell\ell_{jj}$ and associated production of $t\bar{t}H \rightarrow t\bar{t}\gamma\gamma$ as a way of discovering a possible intermediate-mass Higgs particle. Argonne physicists are also contributing to the joint SDC simulation program (SDCSIM), particularly the parametrized shower simulation programs. A major workshop on Detector Performance was held at SSCL at the end of May. it provided a time for all those doing simulations of the detector to meet together, as is usually not possible during working group meetings when other meetings are being held in parallel.

Argonne physicists have served on task forces to recommend technical choices or parameters for SDC. these include the Calorimeter Shape, Compensation, and Tracking Materials task forces. Argonne physicists' participation in the management of SDC now includes chairing an Executive Board subcommittee to recommend the structure and personnel for the top management of SDC in the next (construction) phase. (L. Price)

B. Compensating Scintillator Plate Calorimetry Subsystem

1. Overview

The period of January 1, 1991 to June 30, 1991 saw considerable progress in this program. The stainless steel frames to be used in casting two test electromagnetic calorimeters were fabricated. The first of these was assembled in late January and used to cast Module 1 in April 1991. The conceptual engineering design of the full calorimeter has been extensively developed and now includes details more usually associated with preliminary engineering. Finite element modeling of the barrel electromagnetic calorimeter has been essentially completed within this baseline concept and is currently being refined and further optimized to reduce structural dead material. Simulations of the physics performance of the calorimeter as a function of transverse granularity and longitudinal sampling, and geometry specific compensation calculations have been carried out and the results incorporated in the current engineering design. The Ruthenium source mapping system has been fully commissioned and used to map tiles for both this subsystem and for the CDF Plug upgrade. Studies using this system of the fiber mechanics and route in the tile were carried out to determine the approach to be used for the tiles to be installed in Module 1. These tiles have been laser cut from the raw sheet material and are awaiting access to milling machines to have grooves cut. This is expected to occur in early July.

Samples of candidate radiation hard scintillator plates have been produced under subcontract by Bicron Corporation to attempt confirmation of their expected performance. These are currently being tested at collaborating institutions (Louisiana State University and Florida State University) and results are expected to be available in July. Finally, the test beam installation at Fermilab, where it is intended to perform beam tests of these EM calorimeters in conjunction with a preshower detector, a shower maximum detector, and a hadron calorimeter fabricated by other subsystem groups, has been partially commissioned. The test table to be used for the first three of these devices was to a large extent designed at Argonne. Fabrication of the test table assembly required for the EM calorimeter itself was initiated in late June. An article on the aspect of the calorimeter simulation work dealing with systematics assessment has been written and was submitted for publication in Nuclear Instruments and Methods. (J. Proudfoot)

2. Simulation Studies

Simulation of candidate calorimeter designs and systematic study of simulation tools have continued to be a central part of the design work for a scintillating tile/WLS fiber calorimeter for SDC. To a large extent, the calculations of this six month period represent refinements of previous calculations, as we increasingly focus on a smaller number of possible detector configurations.

First, we undertook systematic simulations, with the CALOR programs, of four configurations for which we have good results from test beams. We identified the sources of systematic uncertainty in the calculations and studied the effect of each on resolution and compensation parameters. Where possible, optimum choices were identified for simulation parameters that can be varied. With optimized parameters, excellent agreement was found with measurement.

We then used the optimized parameters to recalculate the performance of our presently-preferred configuration with lead absorber in the electromagnetic and first hadronic sections, and iron as the absorber in the final hadronic section. Calculations were made for 10, 30, and 75 GeV.

Finally, calculations have been made for a number of proposed variations in the calorimeter configuration. These include varying the thickness of both lead and iron plates and varying the boundary (in interaction lengths) between the lead and iron calorimeter sections. Because others have suggested an all-iron solution for the hadronic calorimeter to improve the magnetic field, this possibility has also been evaluated. The all-iron

configuration gives substantially worse resolution (in particular a large constant term in the resolution), as well as worse compensation. (P. Job/L. Price)

3. Barrel Calorimeter Engineering

a) Design

The design of the SDC barrel calorimeter has gone through three major iterations during this reporting period. These design steps have been taken to compensate for changes dictated by both the physics simulation studies and the necessity for reducing the overall cost of the detector. The design as shown in Fig. 30 represents the latest geometry.

b) Barrel EM Analysis

An FEM model of the EM portion of the barrel was completed and discussed in the previous report, but further work has been done on that model during the last six months. The latest version of the model allows for an optimization study of the support components, and also gives more definitive data on the stresses applied to the cast lead plates. It has been a design goal to minimize the stresses imparted to the lead due to its long term creep characteristics.

Figures 31 and 32 are representative cases showing maximum stresses expected in both the lead plates and the structural bulkheads. This data has led to some customization of bulkhead thicknesses based on position and applied loads:

Bulkhead	Thickness
1-22	1.00 mm
23-24	2.00 mm
25	3.17 mm
26-28	2.00 mm

c) Test Beam Prototype Module

During this reporting period the first of two test beam modules was successfully cast using molds designed and constructed by Westinghouse Science and Technology Center, one of our industrial collaborators. The results of the first casting are shown in Fig. 33.

Some problems were encountered in the construction of the first frame due to distortions created by the welding of the support bulkheads to the front and rear plates.

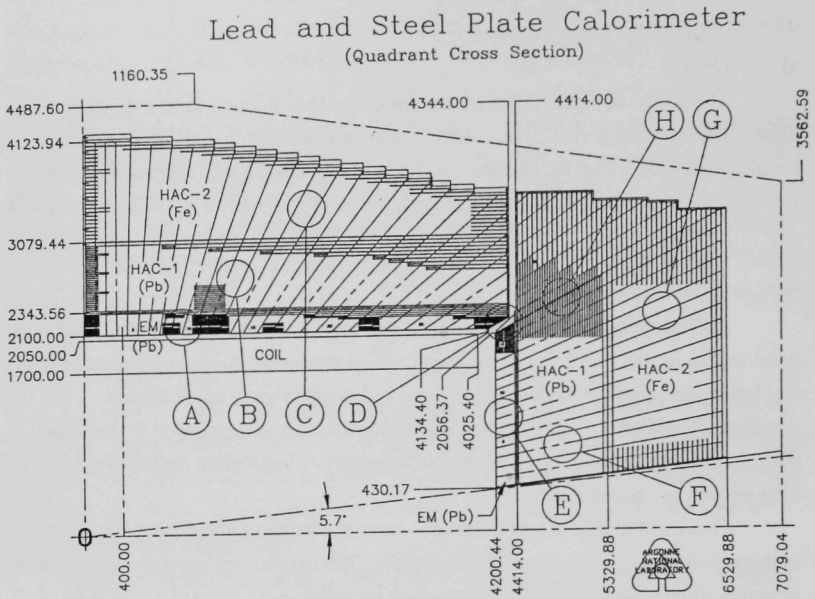

Fig. 30. The latest design of the SDC barrel calorimeter. The internal structure of cross sections A-H are as follows:

A. Barrel EM structure consisting of 10 mm cells with 5.5 mm lead absorber and 4.5 mm scintillator spaces.
B. Barrel HAC-1 section consisting of 20 mm cells with 15.5 mm of load absorber plates and 4.5 mm scintillator spaces.
C. Barrel HAC-2 section consisting of 40 mm cells with 35.5 mm steel absorber plates and 4.5 mm scintillator spaces.
D. Barrel to end cap transition showing 7 cm gap and support structure for end cap end section.
E. End cap EM section consisting of 15 mm cells with 10.5 mm lead absorber plates and 4.5 mm scintillator spaces.
F. End cap HAC-1 section consisting of .25 mm cells with 20.5 mm lead absorber plates and 4.5 mm scintillator spaces.
G. End cap HAC-2 section consisting of 50 mm cells with 45.5 steel absorber plates and 4.5 mm scintillator spaces.
H. End cap stiffener plate that will carry longitudinal magnet coil decentering forces.

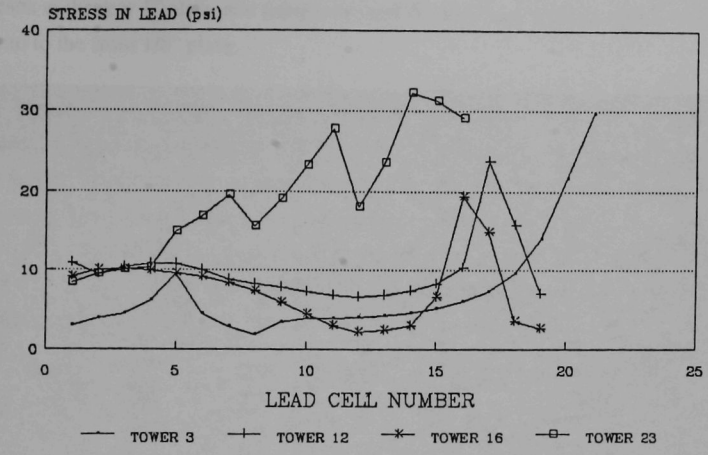

Fig. 31. Maximum stresses in the SDC barrel calorimeter lead plates (12 o'clock position).

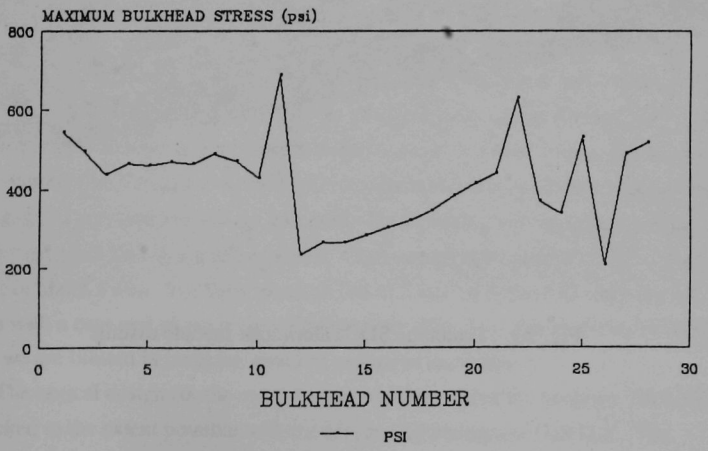

Fig. 32. Maximum stresses in SDC barrel calorimeter bulkheads (12 o'clock position).

Fig. 33. Prototype SDC calorimeter module casting.

This will be corrected on Module 2 by reducing the amount of weld used to attach the bulkheads to the rear 1" plate, and using a tab and slot mechanical attachment of the bulkhead to the front 1/8" plate.

d) Test Beam Setup and Fixturing

Work was completed on the support stand and manipulator for positioning the two prototype EMC modules in the Fermilab MP test beam. The original design was completely redone to reduce the overall cost of the system. The ancillary equipment is now being incorporated into the support stand. (N. Hill)

4. Optical System Development

We completed the tile mapping and measurement facility which was begun last year. It consists of a focused electron beam, trigger scintillators, a two dimensional motor driven frame, electronics, and data acquisition and analysis programs. This facility was used to evaluate many different tile-fiber configurations. We found two configurations which produced more light output than the others and reasonably uniform response. We have chosen one of these to go into production for the EM test module on the basis of fiber routing for ease of assembly of the calorimeter. The test calorimeter scintillation tiles were laser cut to size and work on grooving the tiles and splicing the fibers has begun.

We have developed a 3 MeV electron beam by utilizing a Ru^{106} source and a spectrometer and focussing system of permanent magnets. At this energy the electrons are approximately minimum ionizing in the first several mm of plastic scintillator. The range is great enough to penetrate a 5 mm thick tile, and a 2 mm thick trigger scintillator, and to give a signal in another thicker trigger scintillator. Multiple scattering in the first 2.5 mm of scintillator is not too serious for our spatial resolution of less than 2 mm. By using two trigger counters in coincidence we eliminate non-local and non-penetrating backgrounds such as gamma rays and low energy electrons. By focussing with quadrupoles and dipoles we get an adequate flux in a small spot size. Commercial sources of Ru^{106} of 1 mCi have a diameter of about 5 mm. We have focussed this to 2 mm by 8 mm full width for all particles with a captured phase space of 200 mm-mr (Fig. 34). The rate is a few hundred Hz, and we are limited in mapping speed by computer dead time.

The optical design for the spectrometer was done using the program TRANSPORT and checked to the extent possible with the Monte-Carlo program TURTLE. The spectrometer consists of two sections, an achromatic bending and focussing section, and a quadrupole doublet final focus section. This arrangement provides momentum selection as well as focussing and demagnification with limited chromatic abberations. The first

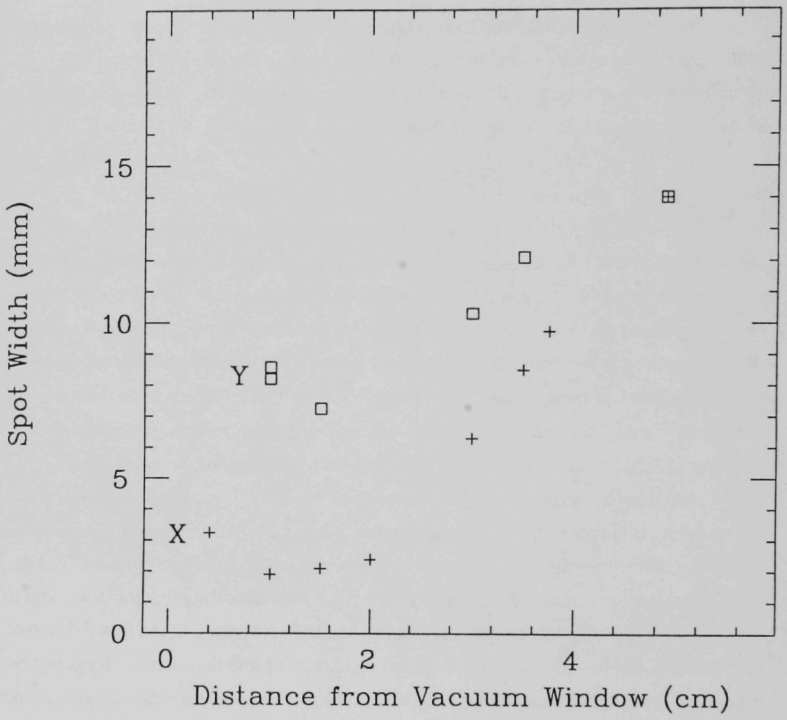

Fig. 34 Width of the beam spot containing all electrons detected with polaroid film. A fit to the beam envelope gives $\varepsilon_x = 200$ mm-mr and $\beta^*_x = 5$ mm.

section utilizes two sector magnets of 45 degree bend each, and a quadrupole between them to make the bend and focus achromatic. The magnets utilize ceramic (ferrite) material with a relatively low B-residual of 2.4 KG. The quadrupoles are made in sectors with no iron and have a gradient of 51. T/M. The worst one has about 5% octupole at the 5 mm radius. The sector magnets have iron flux returns and magnetic poles. The field is about 1.7 KG. Most of the beam transport is in vacuum to limit multiple scattering. The system may be patented by DOE.

We calibrate the number of photoelectrons per minimum ionizing particle by using a LED pulser with a fiber to the same photocathode as the fibers from the tile. Since the variation in pulse height due to variation in light output from the LED is small compared to the variation due to photostatistics, we find the number of photoelectrons at a given pulse height from the square of mean/sigma. This method has been evaluated over a range from 0.6 to 10.2 photoelectrons by means of neutral density filters and has been found to be consistent. The pulse height depends on high voltage, phototube gain, etc. but the number of photoelectrons for a given setup is almost constant for each photocathode. For a good tile-fiber unit we have the number of photo-electrons for two phototubes, and we plan to investigate more.

PHOTOCATHODE EFFICIENCY

Tube	Stages	Typical N Photoelectrons
Amperex 2230	12	1.9
EMI 9839	12	3.0
Hammamatsu R580	10	?
Phillips 2081 green ext.	10	?

We have not been able to investigate 10 stage tubes reliably so far due to the broadening effects of amplifier noise. We have used a special LED pulser system developed at Argonne for CDF. By impedance matching, using absorbing resistors, etc. the complete pulse is less than 100 ns long and low voltages are used which do not damage the LED.

Much of the 3 MeV mapping beam time was shared with the CDF end plug upgrade. This working together has been beneficial for both projects. We have also done some tests of shower max prototypes for SDC and ZEUS.

We have tried a number of combinations of tile and fiber:

Thickness	Configuration	Wrapping	PE
2.5 mm	RH4, two straight fibers, mirrored ends	white paper	1.0-1.1
2.5 mm	Styrene, 4 U fibers, bends outside	white paper	1.65-2.0
5 mm	SCSN38, two straight fibers, mirrored ends	white paper	1.7
2.5 mm	RH4, U fiber, 2.8 M clear spliced on	alum. mylar	2.5
2.5 mm	RH4, U fiber, 2.8 M clear	white paper	1.66
2.5 mm	RH4, U fiber, 2.8 M clear	black tedlar	0.9
2.5 mm	RH4, U fiber, 60 degree beveled edges, 2.8M	alum. mylar	1.75
2.5 mm	RH4, 2 fibers with 4 ends to phototube 2.8 M	alum. mylar	2.0
2.5 mm	RH4, one loop fiber, 2.8 M clear	alum. mylar	3.0

We have also looked at relative outputs of some scintillator materials.

Scint	Splice	Clear Fiber	Groove	Mylar Side	Counts ADC	PE
RH1	ANL	2.8M	LSU	?	90	1.64
RH1	FANL	2.5	LSU	?	98	1.78
RH4	ANL	2.8	LSU	?	119	2.16
Styrene	FNAL	2.5	FNAL-SPI	A	140	2.54
PVT	FNAL	2.5	FNAL-SPI	A	300	5.45
PVT	FNAL	2.5	FNAL-3D	B	240	4.36

It was later determined that most of the difference between the PVT tiles was due to a bad fiber splice and that the side of the mylar used doesn't matter.

Early in June we continued studies of the one-loop design with the fibers coming out the top surface of the tile. Our hope was to build this with no glue whatsoever because of the troubles encountered by CDF with glue on their fibers and because of the non-radiation hardness of some epoxies. We tried to use purely mechanical splints to reinforce the splice between waveshifter and clear fibers. We began studies of masking the reflected light from the aluminized mylar wrap in order to get uniform response. It was found that tiles of this design had a decaying light output with a 1/e time of 10 days.

After numerous tests of the time stability of the optical fibers, we found the problem occurred only in splices under mechanical stress. We tested the light transmission of Kuraray clear fiber, Bicron BCF-91a and fibers made up of alternating segments of these spliced together. Eventually, two tiles were tested with steel hypodermic tubing glued over the splices for reinforcement. These showed no decay over time during the rest of the month. The external routing is shown in Fig. 35.

The masking studies indicate that two small black areas on one side only of the reflective wrap will produce most of the desired uniformity. The final masking design will depend on the final fiber splicing quality, the laser cutting on the edges of the tiles, and the 3-D geometry chosen for the groove where the fibers exit the tile and are routed on top of the tile between the plates of the calorimeter. The unmasked response is shown in Fig.36.

The actual tiles for the EM test beam module were cut at Laser Services in Massachusetts from RH4 material supplied by Bicron. The cutting service had to experiment extensively in order to cut this new material with an optical surface at right angle to the larger tile dimensions. They had previously been very successful with SCSN81 scintillator for the ZEUS calorimeter. They also had to anneal our material at a lower temperature, 125 F, to prevent eventual crazing. The tiles have a small ridge at the corner from the laser cutting. A few of the tiles have some surface damage due to splattered molten plastic from the cutting process. They are coated with an emulsion, ("Emulsitone") before cutting to minimize scratches during handling. It is time consuming to wash off this emulsion by hand before grooves can be cut in the tiles, but we do not want soap or emulsion to accumulate in the grooves. The transverse dimensions are 0.0 to 0.5 mm smaller than nominal, which is good for inserting tiles into the casting.

The material supplied was measured and weighed at Argonne and found to have an average thickness of 2.61 mm and rms deviation of 3.6 %. Only enough scintillator material was available at this time for 6 of the 10 towers of the test calorimeter. Half the tiles were sent to LSU for grooving and half to Fermilab. They were selected on the basis of tile weight which correlates with thickness.

About 10 % of the fibers for the EM test beam module were spliced, splinted, and polished at Fermilab. The one fiber tested so far in an actual tile gave 13% more light than our test fibers spliced at Argonne. (The Argonne splicer supplied by Rockefeller had a broken quartz tube and only an oversize replacement was immediately available.)

A fiber assembly testing box is being built. It will read the 8 ends of 4 fiber assemblies simultaneously, for immediate spotting of problems. PIN diodes are used with current to voltage amplifiers and a 12 bit 8 channel adc in a PC computer. A length of WLS fiber roughly equal to the length to be in the tile is illuminated by uv light. The box

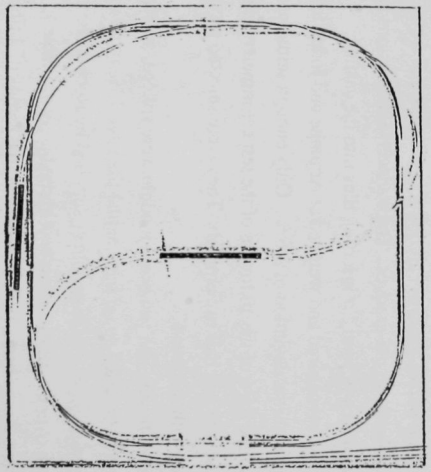

Fig. 35. A tile from EM Tower 2, Layer 29. The loop fiber path in the tile is shown as well as the external fiber routing. The steel ferrules are used to reinforce the splices between wave shifter fiber and clear fiber.

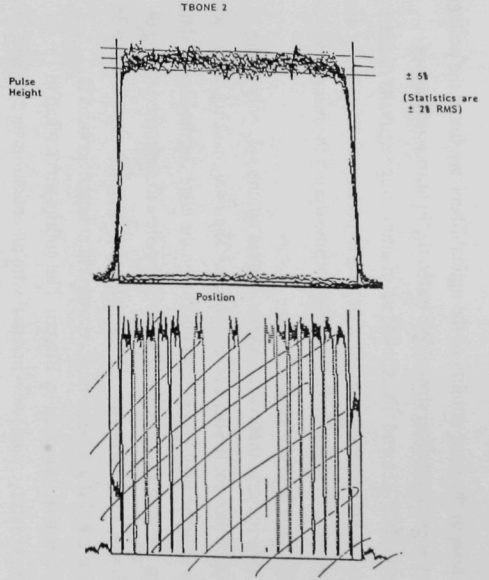

Fig. 36. Example of a tile-fiber map for a configuration which has good uniformity with no mask but which requires fibers to be threaded through the calorimeter. We have chosen a different configuration which is easier to assemble.

was tested with one fiber and performed as expected except that the clamps for the fibers were too difficult to use for mass-production testing. New clamps are being designed and built. (D. Underwood)

5. Test Beam Plans for Scintillating Tile E-M Calorimeter

The scintillating tile EM calorimeter prototype constructed by the Argonne High Energy Physics Division and Westinghouse Science and Technology Center will be studied in a test beam at Fermi National Accelerator Laboratory. Testing will be done as part of an overall calorimeter subsystem study including the EM calorimeter, a scintillating fiber pre-shower detector, a scintillating tile shower maximum detector embedded in the EM calorimeter, and a prototype scintillating tile, iron absorber hadron calorimeter. The support stand and EM calorimeter module configuration is shown in Fig. 37.

The test beam experiment is located in the MP line of the Meson Area at Fermilab. The measurement goals for the various detectors are given in the following list.

Pre-Shower and Shower Maximum Detector

- The e/π separation capability of the detectors for varying amounts of material preceding the detectors will be studied.
- The energy dependence of the e/π separation will be measured.
- Alternative readout technologies for the detectors will be evaluated.

EM Calorimeter

- The feasibility of using optical fibers for readout will be determined.
- The resolution, linearity, and uniformity of response across tower and module boundaries of the EM calorimeter will be measured.
- A study will be done to determine the precision with which the absolute calibration of the detector can be maintained using a radioactive source to sample varying depths in the calorimeter.
- The radiation hardness of the EM calorimeter and readout fiber system will be determined.
- Front-end electronic prototypes for pipeline readout and triggering from the scintillation calorimeter will be tested.

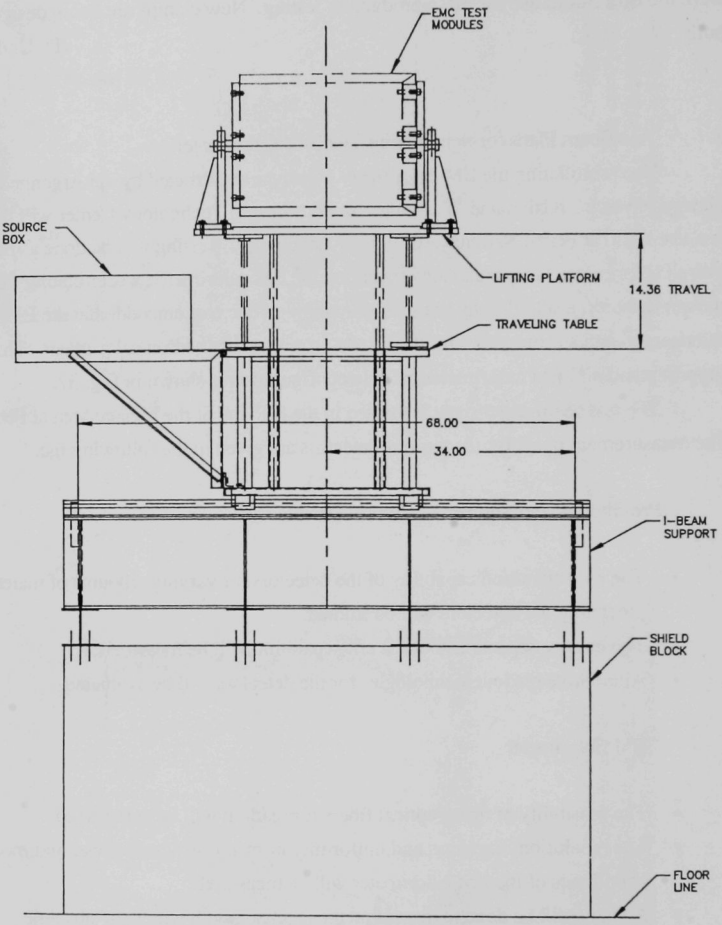

Fig. 37 Schematic drawing of the EM calorimeter and support stand for beam testing at Fermilab. Units of length are in inches. The beam direction is out of the page and is centered on the crossed dashed lines.

Hadron Calorimeter

- The ratio of electromagnetic-to-hadronic response of the calorimeter will be measured. It is desirable to have this ratio close to 1.0.
- The resolution and linearity of the calorimeter will be measured.

The 1991 fixed target run at Fermilab began at the end of June. The beam will be brought into the MP area in mid to late July. The pre-shower detector has arrived at Fermilab and was being installed at the close of June. We expect the EM calorimeter to be ready for installation in the test beam by the end of July. Tuning of the beam line magnets and check out of the beam diagnostics will occur over a two week period as soon as the beam is brought into the experimental area. We anticipate that in August we will begin data taking for the purpose of accomplishing these measurements.

(R. Wagner)

C. Radhard Electronics R&D

During the first half of 1991 the efforts in the radhard electronics testing focused on evaluating UTMC's UTDR 1.5 micron rad-hard CMOS/bulk process and Hughes Aircraft's CMOS/SOS. Neutron irradiations of up to 10^{14} neutrons/cm^2 were performed at the Dynamitron Fast Neutron Generator (FNG). This neutron source is characterized by a energy spectrum similar to the expected spectrum at the SSC which peaks at around 1 MeV. Other advantages at the FNG are the easy port access and low quantities of thermal neutrons, allowing for short de-activation time of experimental apparatus. All ionizing irradiation have been done at the Cobalt-60 source in the Biology and Medical Division, where dose rates of up to 2 MRad(Si)/hour allows us to simulate 10 SSC-years in one day. Total dose effects of irradiation up to 10 MRad(Si) have been studied.

The results of our radiation damage experiments have been very encouraging with no degradation of performance for neutron irradiations. The damage from ionizing irradiation was negligible for 1 MRad(Si) for both the CMOS/bulk and CMOS/SOS while the performance was severely degraded for the CMOS/SOS at 10 MRad(Si) with threshold shifts of several volts and 30 percent degradation in transconduction. The CMOS/bulk,

however, performed very well even after 10 MRad(Si) with 200 mV worst case threshold shift and no change in transconductance.

We have used our good working relationships with the radiation sources at ANL to facilitate other experimenters interested in radiation damage research. Optical fibers and Cs-I scintillators have been irradiated at the Biology Division's Cobalt-60 source. In order to test the radiation damage on scintillating tiles our familiarity with the sources at ANL have been used to develop a testing program at the Cobalt-60 source in the Chemistry Division, which has a higher dose rate and easier access for larger samples needing high total dose.

(J. Dawson)

VI. PUBLICATIONS

A. Journal Publications, Conference Proceedings, Books

A Beam Profile Monitor for Small Electron Beams
J. Norem
Rev. of Sci. Instr. 62, 1464 (1991)

Comparison of Spin Asymmetries & Cross Sections in Production by 200-GeV Polarized Antiprotons and Protons
A. Yokosawa and E-704 Collaboration
Phys. Lett. B261, 201 (1991)

First Results for the Two-Spin Parameters A_{LL} in ρ° Production by 200-GeV Polarized Protons and Antiprotons
A. Yokosawa and E-704 Collaboration
Phys. Lett. B261, 197 (1991)

Comparison of Bottom Quark Production Rates in ISAJET with a Full QCD 2-3 Calculation
E. L. Berger, E. Kuebel, M. Pundurs (ANL/HEP), F. E. Paige (BNL)
Phys. Rev. D43, 767 (1991)

Theory of the Anisotropic Ferrite Wakefield Accelerator
S. Mtingwa (ANL/HEP)
Phys. Rev. A43, 5581 (1991)

Hard-Scattering Scaling Laws for Single-Spin Production Asymmetries
D. Sivers (ANL/HEP)
Phys. Rev. D43, 261 (1991)

Theory of the Anisotropic Ferrite Wakefield Accelerator II: Higher Order Modes
J. T. Chiu and S. K. Mtingwa (ANL/HEP)
Phys. Rev. A43, 5590 (1991)

Measurement of Deflection Mode Dampening in an Accelerator Structure
E. Chojnacki, W. Gai, C. Ho, R. Konecny, S. Mtingwa, J. Norem, M. Rosing, P. Schoessow, and J. Simpson (ANL/HEP)
Journal of App. Phys. 66 (9), 6257 (1991)

Measurements of $\Delta\sigma_L$(np) between 500 and 800 MeV
M. Beddo, G. Burleson, J. Faucett, S. Gardiner, G.Kyle (New Mexico State); R. Garnett, D. Grosnick, D. Hill, K.Johnson, D. Lopiano, Y. Ohashi et al. (ANL/HEP)
Phys. Lett. B258, 24 (1991)

The W-Top Background to Heavy Higgs Production
G. A. Ladinsky and C. P. Yuan (ANL/HEP)
Phys. Rev. D43, 789 (1991)

Baryon Number Violation with New Improved Instantons
P. B. Arnold (ANL/HEP), M. P. Mattis (LANL)
Phys. Rev. Lett. 66, 13 (1991)

Topological Fluctuations in Lattice QCD: An Exploratory Study
J. Kogut (Univ. of Illinois), D. Sinclair (ANL/HEP), M. Teper (All Souls College and Univ. of Oxford)
Nucl. Phys. B348, 178 (1991)

W and Z. Production at Next-to-Leading Order: From Large q_t to Small
P. B. Arnold and R. P.Kauffman
Nucl. Phys. B349, 381 (1991)

Measurement of the W Boson Mass at 1.8 TeV pp Collisions
L.Nodulman
Phys. Rev. D43, 2070 (1991)

Interference Effects in $K\eta$ and $K\eta'$ Decay Modes of Heavy Mesons
H. J. Lipkin
Phys. Lett. B254, 247 (1991)

Multiparameter Associative Generalizations of Canonical Commutation Relations and Quantized Planes
D. B. Fairlie and C. K. Zachos
Phys. Lett. B256, 43 (1991)

Top Quark Search in the Electron + Jet Channel in Proton-Antiproton Collisions at $\sqrt{s}$ = 18 TeV
L. Nodulman and the CDF Collaboration
Phys. Rev. D43, 664 (1991)

Evidence for Multiple Scattering of High Energy Partons in Nuclei
M. Corcoran, M. W. Arenton, W. R. Ditzler, T. H. Fields, M. Harrison, A. Kanofsky, R. Gustafson, L. Cormell, H .F. Chen
Phys. Lett. B259, 209 (1991)

Flow-Rate Independent Gas-Mixing System for Drift Chambers Using Solenoid Valves
K. Sugano
Nucl. Instr. and Meth. A301, 454 (1991)

B. Papers Submitted for Publication and ANL Reports

On Glueballs & Topology in Lattice QCD with Two Light Flavors
K. M. Bitar, R. Edwards, U. M. Heller, A. D. Kennedy (SCRI), T. A. DeGrand (Univ. of Colorado); S. Gottliev, A. Krasnitz (IN Univ.); J. B. Kogut, R. L. Renken (Univ. of IL); W. Liu, P. Rossi (Thinking Machines Corp., Cambridge, MA); M. C. Ogilvie (WA Univ.); D. K. Sinclair, K. C. Wang (ANL/HEP); R. L. Sugar (Univ. of CA); M. Teper (Univ. of Oxford); D. Tousaint (Univ. of AZ)
ANL-HEP-PR-91-06
Submitted to Phys. Rev. D

Multiparameter Deformations of GL(N) and Jordan-Schwinger Constructions
S. Vokos
ANL-HEP-PR-91-07
Submitted to the Journal of Mathematical Physics

High-x_T Single-Spin Asymmetry in ρ° Production at $x_F = 0$ by 200-GeV Polarized Antiprotons and Protons
A. Yokosawa
ANL-HEP-PR-91-09
Submitted to Phys. Rev. Lett.

Large-x_F Spin Asymmetry in μ° Production by 200-GeV Polarized Protons
A. Yokosawa and E-704 Collaboration
ANL-HEP-PR-91-10
Submitted to Phys. Rev. Lett.

Improved beta detection efficiency with granular aluminum superconducting strips
A. Gabutti (ANL/HEP), K. E. Gray (ANL/MSD), G. M. Pugh and R. Tiberio, (National Nanofabrication Facility, Ithaca, NY)
ANL-HEP-PR-91-12
Submitted to Nuclear Instruments and Methods A

Higgs-Boson p_T in Gluon Fusion
R. Kauffman
ANL-HEP-PR-91-21
Submitted to Phys. Rev. D

Modelling of the Transverse Mode Suppressor for Dielectric Wake Field Accelerator
W. Gai and C. Ho
ANL-HEP-PR-91-22
Submitted to Journal of Applied Physics

Gauge Propagator Contribution to High-Energy Baryon Number Violation
P. Arnold and Michael P. Mattis
ANL-HEP-PR-91-23
Submitted to Mod. Phys. Lett. A

Semi-Inclusive Deeply Inelastic Scattering at Electron-Proton Colliders
R. Meng, (ANL/HEP), F. Olness, (Univ. of Oregon), D. Soper (CERN)
ANL-HEP-PR-91-24
Submitted to Nucl. Phys. B

Can We Use Asymptotic Analytic Amplitude Analysis in the Energy Region 5-1800 GeV
M.M. Block (Northwestern University) and A.R. White (ANL/HEP)
ANL-HEP-PR-91-38
Submitted to Phys. Lett. B

Instability of Hot Electroweak Theory: Bounds on m_H and m_t
Peter Arnold and Stamatis Vokos
ANL-HEP-PR-91-39
Submitted to Phys. Rev. D

A Neutron Hodoscope for Medium Energy np Scattering Experiments
R. Garnett, D. Grosnick, K. Johnson, D. Lopiano, Y. Ohashi, A. Rask, T. Shima, H. Spinka, R. Stanek, D. Underwood, A. Yokosawa (ANL/HEP); M. Beddo, G. Burleson, J. A. Faucett, G. Kyle (New Mexico State Univ.); M. Devereux, G. Glass, S. Nath (Texas A&M); J. J. Jarmer, S. Pentilla (Los Alamos National Lab); R. Jeppesen (Univ. of Montana); G. Tripard (Washington State University)
ANL-HEP-PR-91-45
Submitted to Nuclear Instruments and Methods A

Analyzing Power in Inclusive μ^+ and μ^- Production at High x_F with a 200 GeV Polarized Proton Beam
A. Yokosawa (ANL/HEP) and E-704 Collaboration
ANL-HEP-PR-91-46
Submitted to Physics Letters

Construction and Beam Test of the ZEUS Forward and Rear Calorimeter
J. Dawson (ANL/HEP); A. Andresen et al. (Univ. of Hamburg); A. Bamberger (Univ. of Freiburg) and the ZEUS Calorimeter Group
ANL-HEP-PR-91-51
Submitted to Nuclear Instruments and Methods

Comparison of CALOR89 Model Predictions with Scintillator Plate Calorimeter Data
P.K. Job, L. Price, J. Proudfoot (ANL/HEP); T. Handler (University of Tennessee); B.L. Bishop and T.A. Gabriel (Oak Ridge National Laboratory)
ANL-HEP-PR-91-52
Submitted to Nuclear Instruments and Methods

The Observation of Underground Muons From the Direction of Cygnus X-3 during the January 1991 Radio Flare
I. Ambats (ANL-HEP); M. Thomson et al. (Oxford University); G.J. Alner (Rutherford-Appleton Lab); D. Benjamin (Tufts University); P. Border (Univ. of Minneapolis)
ANL-HEP-PR-91-57
Submitted to Physics Letters B

Delepton Production by Protons on Nuclei and the Partonic Origin of Depletion at Small Momentum Fraction
K.E. Lassila (ANL/HEP and Iowa State), U.P. Sukhatme (U. of I.), A. Harindranath (Ohio State), and J.P. Vary (Iowa State)
ANL-HEP-PR-91-58
Submitted to Phys. Rev. C

A Monte Carlo Program for Generating QED Radiative Decay W and Z Events
Robert G. Wagner
ANL-HEP-PR-91-59
Submitted to Computer Physics Communications

Design and Construction of the ZEUS Barrel Calorimeter
M. Derrick, D. Gacek, N. Hill, B. Musgrave, R. Noland, E. Petereit, J.Repond, R. Stanek (ANL/HEP), K. Sugano (Inst. of Particle Physics, Univ. of California-Santa Cruz)
ANL-HEP-PR-91-30
Submitted to Nuclear Instruments and Methods

The Odderon Versus a New Threshold - Implications for Experiments and from Confinement in QCD
Kyungsik Kang (Brown University) and Alan R. White (ANL/HEP)
ANL-HEP-PR-91-32
To Be Published in Phys. Lett. B

C. Papers or Abstracts Contributed to Conferences

Direct Photon Production in Polarized PP Collisions
E. Berger and J. Qiu (ANL/HEP)
ANL-HEP-CP-91-01
Proceedings of the Polarized Collider Workshop, Pennsylvania State University, University Park, PA; 15-17 November 1990, edited by J. Collins, S.F. Heppelman, and R.W. Robinett. (AIP Conf. Proc. Series No. 233, New York, 1991), p. 162

Transverse Spin Observables in Hadron-Hadron and Hadron Nucleus Collisions
D. Sivers (ANL/HEP)
ANL-HEP-CP-91-02
Polarized Collider Workshop, Pennsylvania State University, University Park, 15-17 November 1990

Recent Results & Future Prospects for the Polarized Beam at Fermilab
A. Yokosawa (ANL/HEP)
ANL-HEP-CP-91-03
Polarized Collider Workshop, Pennsylvania State University, University Park, PA; 15-17 November 1990

Advantages of Polarization Experiments at RHIC
D. Underwood (ANL/HEP)
ANL-HEP-CP-91-11
Proceedings of the Polarized Collider Workshop, AIP Conf. Proc. 223, Particles and Field Series 42, 321 (1991)

A Design Study of a Cast Lead Electromagnetic Calorimeter for the Solenoidal Detector Collaboration at SSC

N. Hill, V. Guarino, J. Nasiatka (ANL/HEP), M. Burke, R. Swensrud (Westinghouse Science and Technology Center)

ANL-HEP-CP-91-18

To be published in the Proceedings of the Third Annual International Industrial Symposium on the Super Collider (IISSC), Atlanta Hilton and Towers, Atlanta, GA (March 13-15, 1991), ed. J. Nonte, Plenum Press, New York

Systematic Effects in CALOR Simulation Code to Model Experimental Configurations

P. K. Job and J. Proudfoot (ANL/HEP), T. Handler, Univ. of Tennessee; T. A. Gabriel, Oak Ridge National Laboratory

ANL-HEP-CP-91-27

Submitted to the Proceedings of Workshop on Detector and Event Simulation in High Energy Physics; 8-12 April 1991; NIKHEF Laboratory, Amsterdam, Netherlands

Quantized Planes and Multiparameter Deformations of Heisenberg and GL(N) Algebras

C. Zachos (ANL/HEP); D. B. Fairlie (Univ. of Durham, England)

ANL-HEP-CP-91-28

Invited talk at the Miami NATO ARW on Quantum Coral Gables, January 11, 1991. To be published in the Proceedings of Coral Gables NATO Workshop, ASI series, Plenum

Radhard Electronics Study for SSC Detectors

T. Ekenberg, J. Dawson, A. Stevens, W. Haberichter (ANL/HEP)

ANL-HEP-CP-91-33

To Be Published in the Proceedings of the Third Annual International Industrial Symposium on the Super Collider (IISSC), Atlanta Hilton and Towers, Atlanta, GA (March 13-15, 1991), ed. J. Nonte, Plenum Press, New York

Accelerating Field Step-Up Transformer in Wake-Field Accelerators

E. Chojnacki, W. Gai, P. Schoessow and J. Simpson(ANL/HEP)

ANL-HEP-CP-91-41

To Be Published in the IEEE 1991 Particle Accelerator Conference Proceedings, San Francisco, CA, May 1991

An Update on Argonne's AWA

M. Rosing, E. Chojnacki, W. Gai, C. Ho, R. Konecny, S. Mtingwa, J.Norem, P. Schoessow and J. Simpson (ANL/HEP)

ANL-HEP-CP-91-42

To Be Published in the IEEE 1991 Particle Accelerator Conference Proceedings, San Francisco, CA, May 1991

Development of Laser Optics of the AWA Photocathode

J. Norem and W. Gai (ANL/HEP)

ANL-HEP-CP-91-43

To Be Published in the IEEE 1991 Particle Accelerator Conference Proceedings, San Francisco, CA, May 1991

A New Kind of Bottom Quark Factory
S. Mtingwa (ANL/HEP), M. Strikman (Univ. of Illinois)
ANL-HEP-CP-91-44
Submitted to the Fourteenth Annual Meeting of the National Society of Black Physicists, Hampton Univ. and CEBAF, April 12, 1991

Status of NP Spin-Dependent Total Cross Sections and Spin-Spin Correlation Parameters
M. Beddo (ANL/HEP)
ANL-HEP-CP-91-47
4th Conference on the Intersections Between Particle and Nuclear Physics Tucson, Arizona May 24-29, 1991 (Yale Univer., Brookhaven Lab., Univ. Manitoba)

Development of a Custom Monolithic Device for Data Acquisition from a Scintillating Calorimeter at the Superconducting Super Collider
T. Ekenberg, J. W. Dawson, R. L. Talaga, A. E. Stevens, W. N. Haberichter (ANL/HEP)
ANL-HEP-CP-91-48
To Be Published in the Proceedings of the Third Annual International Industrial Symposium on the Super Collider (IISSC), Atlanta Hilton and Towers, Atlanta, GA (March 13-15, 1991), ed. J. Nonte, Plenum Press, New York

Fermilab Polarized Beam Experiments - π° and η Production Results
A. Yokosawa
ANL-HEP-CP-91-53
Submitted to the Proceedings of the 4th Conference on the Intersections Between Particle and Nuclear Physics, 27-29 May 1991 Tucson, Arizona (Brookhaven National Lab., TRIUMF)

Light Quarks and the Pomeron in QCD
A.R. White
ANL-HEP-CP-91-54
Presented at the 4th Blois Workshop on Elastic and Diffractive Scattering, Isle of Elba, Italy, May 1991

From Knots to Quantum Groups (and Back)
R. Kauffman (ANL/HEP)
Proceedings of the Argonne Workshop on Quantum Groups, (World Scientific Publishing Co.), edited by D. Cartwright et al., pps. 1-32 (1991)

A New Approach to Chiral Fermions on the Lattice
G. Bodwin (ANL/HEP) and E. Kovacs (FNAL)
Nucl. Phys. B (Proc. Suppl.) Proceedings of the Lattice '90 Conference 20, 20, pp. 546-550 (1991)

Paradigms of Quantum Algebras
C. Zachos (ANL/HEP)
Proceedings of the Symmetries in Science V, edited by B. Gruber et al., pps. 593-609 (1991)

Parallelization of a Radiation Transport Simulation Code on the BBN TC2000™ Parallel Computer
E. May (ANL/HEP), W. Celmaster (BBN Advanced Computers, Inc.),
Proceedings of Supercomputing '90, (1991 IEEE Computer Society), pps. 448-453 (1991)

Quantum Deformations
C. K. Zachos (ANL/HEP)
Proceedings of the Argonne Workshop on Quantum Algebras, (World Scientific Publishing Co.), edited by T. Cartwright et al. (1991)

Scientific Research in the Soviet Union
S. K. Mtingwa (ANL/HEP)
Proceedings of the 13th Annual Meeting of the National Society of Black Physicists, Southern University, Baton Rouge, LA (1991)

Computer Simulations of New Dielectric Accelerator Devices
K. C. D. Chan (LANL), P. Schoessow (ANL/HEP)
Proceedings of the 1990 Linear Accelerator Conference, p. 736 (1991)

D. Technical Notes

SDC Hadronic Mass Resolutions in Z and Z' Decays
R. E. Blair, L. E. Price, and H. J. Trost (ANL/HEP)
ANL-HEP-TR-91-13

1990 Results with Polarized Protons and Antiprotons (E-704)
A. Yokosawa (ANL/HEP)
ANL-HEP-TR-91-16
To appear in the "Fermilab Report"

Fast Shower Simulation Based on Gauss' Law
H.-J. Trost
ANL-HEP-TR-91-17

Estimation of Hadronic and EM Resolution for Scintillator Plate Calorimeter Configurations
P. K. Job and J. Proudfoot (ANL/HEP)
ANL-HEP-TR-91-19

On Implications of e/h = 1
L. Nodulman
ANL-HEP-TR-91-20

Simulation of the Passage of Muons Through the Rock Overburden into the Soudan 2 Cavern
Hans-Jochen Trost
ANL-HEP-TR-91-56

AGN-8 Linac Cooling
M. Rosing

AGN-9 Solenoid Coils
M. Rosing

AGN-10 Field Mapping Ideas
M. Rosing

CDF-1335 Estimation of the Equivalent Radiator Thickness for Radiative W Decay
R. Wagner

CDF-1350 BO Cosmic Ray Checkout of the Preradiator
S. Kuhlmann

CDF 1362 Test Beam Results from Prototype Scintillating Tile Calorimeters with Fiber Readout
R. Hagstrom et al.

CDF 1392 Single-Cut Statistical Background Subtraction
S. Kuhlmann

CDF-1396 W. Transverse Mass Versus 6 bunch Luminosity
L. Nodulman

CDF-1408 $\Lambda, \overline{\Lambda}$ and K_S Production with Electrons
F. Ukegawa, A. B. Wicklund

CDF-1431 Jet Studies in the Photon Sample, Volume I
S. Kuhlmann, L. Nakae

CDF-1432 CES Response and Chisquared for 1990 Testbeam Electrons
R.. Harris, R. Blair, S. Kuhlmann

CDF-1435 Photon/Electron Longitudinal Shower Differences (A Simple Approach)
R. Blair

CDF-1436 A GEANT Simulation of the CES
R. Blair

CDF-1439 K*(890) and Phi (1020) Production with Electrons
A. B. Wicklund, F. Ukegawa

CDF-1467 Trigger and Physics Cross Sections for the 1991 Run
R. Blair, S. Kuhlmann, et al.

CDF 1469 A Study of Hadron Showers for the Electron Analysis
F. Ukegawa, A. B. Wicklund

CDF-1470 CES Calibration Studies Using BO Electrons
S. Kuhlmann

CDF-1489 A Monte Carlo Program for Generating QED Radiative Decay W and Z Event
R. Wagner

CDF-1490 CDF Data Storage and Analysis Modifications
R. Blair, S. Kuhlmann, L. Nodulman, et al.

CDF-1492 Fragmentation Issues in the Bottom quark Cross Section Measurement
J. Proudfoot, F. Ukegawa, A. B. Wicklund

PDK-462 Soudan 2 Nucleon Decay Experiment - Quarterly Report
D. Ayres

PDK-463 Decision of the U.K. Collaboration Meetings
D. Ayres, N. West

PDK-465 Proposal for A Long Baseline Neutrino Oscillation Experiment Using the Soudan 2 Neutrino Detector
M. Goodman

PDK-466 Chapter 3 Long-Baseline Oscillation Experiments
M. Goodman

PDK-468 Soudan 2 Nucleon Decay Experiment - Quarterly Report
D. Ayres

PDK-472 Choosing Between Two Alternate Hypotheses...
T. Fields

PDK-474 Determination of pion intranuclear rescattering rates in ν_μ–Ne versus $\nu\mu$-D interactions for the atmospheric ν flux
M. Derrick and B. Musgrave

DC-91-00013 Estimation of Hadronic and EM Resolution for Scintillator Plate Calorimeter Configurations
P. K. Job and J. Proudfoot

SDC-91-00014 Central Calorimeter Configuration - A Study Report to the SDC Technical Board
T. Kirk and B.Wicklund

WF-158 Bremsstahlung Radiation Electron Beam Monitoring System (BREMS)
J. Norem

WF-159 Numerical simulations of beam break up (BBU) effects in a dielectric wake field tube
W. Gai

WF-160 Another Plasma - Wake Field Experiment?
E. Chojnacki

WF-161 Multipactoring in the AWA
M. Rosing

VII. COLLOQUIA AND CONFERENCE TALKS

P. Arnold

"Review of Anomalous B Violation"
Aspen Winter Workshop, Aspen, CO (January 1991)
Purdue University (January 1991)
New York University (February 1991)
Univ. of Chicago (March 1991)
Duke Univ. (February 1991)
Univ. of Connecticut, Storrs (April 1991)

"Anomalous B Violation and Improved Instantons"
Fermilab (February 1991)
Univ. of Michigan (February 1991)
Univ. of California, Berkeley (February 1991)
Univ. of Washington, Seattle (February 1991)
CERN, Geneva (February 1991)

"W and Z Production at Next-to-Leading Order: from small p_T to Large"
CERN, Geneva (February 1991)

"Instability of Hot Electroweak Theory: Bounds on m_H and m_t"
Northwestern Univ. (May 1991)
Ohio State Univ. (May 1991)

E. Berger

"Quantum Chromodynamics and Collider Physics"
Michigan State University Lecture Series (January 1991)

"Prompt Photon Production at Collider Energies"
Fermi National Accelerator Laboratory (March 1991)

M. Derrick

"Design and Construction of the ZEUS BCAL"
Zakopane, Poland (June 1991)

P. K. Job

"Evaluation of Calor Code System Capabilities in the Design of an SSC Calorimeter"
SSC Laboratory, Dallas, TX (May 1991)

R. Kauffman

"W and Z Production: From Large p_T to Small"
Florida State Univ. (January 1991)
Northwestern Univ. (February 1991)
Fermilab (February 1991)

"Higgs p_T"
SSC Symposium, Madison, WI (February 1991)

T. Kirk

"IISSC Symposium Program"
IISSC 3rd Annual Symposium, Atlanta, GA (March 1991)

"Cost Estimating the SDC Central Calorimeter"
Fermilab (May 1991)

S. Kuhlmann

"New Particle Searches at CDF"
2nd International Symposium on Particles, Strings, and Cosmology, Northeastern University, Boston, MA (March 1991)

E. May

"Summary of Remote Computing and Networking"
Workshop on Computing for SDC: Rutgers University (May 1991)

R. Meng

"Can Perturbative QCD Explain Sea Quark Distributions?"
ANL (June 1991)

S. Mtingwa

"Combining a Linear Collider with a B-Factory"
UCLA Workshop on Novel Flavor Factories, Los Angeles, CA (February 1991)

"Science, Technology and the African"
AT&T Bell Labs, Murray Hill, NJ (February 1991)
Princeton Univ. (February 1991)

"A New Kind of Bottom Quark Factory"
CEBAF, New Port News, VA (April 1991)

M. Rosing

"The Argonne Wakefield Accelerator Project"
Fermilab (February 1991)

H. Spinka

"Summary of Parallel Session Talks on Spin"
Intersections of Particle and Nuclear Physics Conference, Tucson, AZ (May 1991)

H.-J. Trost

"Simulation Studies for Experimentation at the SSC"
University of Texas at Dallas, Richardson, TX (April 1991)

A. White

"A Collider Diffractive Threshold, Hadronic Photons, and Sextet Quark"
Fermilab (January 1991)

"Diffractively Produced Massive Photon Pairs, A Signal for New Physics?"
Micro-Plug Workshop, Fermilab (February 1991)

"Sextet-Quark Physics"
Sextet-Quark Mini-Workshop, Fermilab (March 1991)

"Light Quarks and the Pomeron in QCD"
4th International Conference on Elastic and Diffractive Scattering (May 1991)

B. Wicklund

"b-Physics at CDF"
Univ. of Michigan (January 1991)
U. C. Riverside (February)

A. Yokosawa

"Fermilab Polarized Beam Experiments π^0 and η Production Results"
4th Conference on the Interactions between Particles and Nuclear Physics, Tucson, AZ (May 1991)

C. Zachos

"Quantized Planes and Deformations of Heisenberg and GL(N) Algebras"
U. Miami, Coral Gables Conference (January 1991)

"Multiparameter Deformations of Heisenberg and GL(N) Algebras"
XXth International Conference on Differential Geometry Methods in Physics, New York City (June 1991)

"Overview of Particle Physics"
Argonne Science & Engineering Research Semester Seminar (February 1991)
Student Research Participation Seminar (June 1991)

VIII. HIGH ENERGY PHYSICS COMMUNITY ACTIVITIES

E. Berger

High Energy Physics Advisory Panel (HEPAP, 1991)

Chairman, Fellowship Subcommittee, Division of Particles and Fields, 1991

International Advisory Committee, 1991 General Meeting of the Division of Particles and Fields, University of British Columbia, Vancouver, Canada, August 1991

Scientific Program Committee, XXVI Recontre de Moriond, "High Energy Hadronic Interactions", Les Arcs, France, March 1991

Parallel Session Coordinator, Fourth Conference on the Intersections between Particle and Nuclear Physics Tucson, Arizona, May 1991

Texas National Research Laboratory Commission's Research and Development Review Subpanel, 1990-1991

Member, Committee on Meetings, American Physical Society

Scientific Advisory Board, Hadron '91, University of Maryland, August 12-16, 1991

International Advisory Committee, DPF Meeting, Fermilab, October 1992

T. Fields

Chair, ATLAS Heavy Ion Accelerator External Safety Review, January 1991

T. Kirk

Program Chairman - 1991 Intl. Industrial Symposium on the Supercollider
RHIC Construction Project Review - committee member
Institutional Board chairman - Solenoidal Detector Collaboration
SDC Central Calorimeter Cost Est. Task Force - Chairman

S. Mtingwa

President-Elect, National Society of Black Physicists
Advisory Committee to President of Malcolm X College, Chicago

H. Spinka

LAMPF Board of Directors

Session Organizer for Spin Parallel Session Talks for Conference on the Intersections of Particle and Nuclear Physics, Tucson, AZ, May 1991

B. Wicklund

Member of International Advisory Committee-Physics in Collision Conference, Colmar 1991

A. Yokosawa

Session Organizer on Polarization Phenomena in High Energy Collisions, XXII International Symposium on Multiparticle Dynamics, September 1991

C. Zachos

Advisory & Organizing Committee of the Coral Gables Workshop on QFT, Statistical Mechanics, Quantum Groups and Topology, Miami , January 1991

IX. HIGH ENERGY PHYSICS RESEARCH PERSONNEL

Administration

T. Kirk
P. Moonier

Accelerator Physicists

W. Gai
S. Mtingwa
J. Norem
M. Rosing
P. Schoessow
J. Simpson

Experimental Physicists

D. Ayres
R. Blair
M. Derrick
T. Fields
M. Goodman
D. Grosnick
R. Hagstrom
P. Job
S. Kuhlmann
D. Lopiano
S. Magill
E. May
B. Musgrave
L. Nodulman
Y. Ohashi
L. Price
J. Proudfoot
J. Repond
H. Spinka
R. Stanek
K. Sugano
R. Talaga
J. Thron
H.-J. Trost
D. Underwood
R. Wagner
A. B. Wicklund
A. Yokosawa

Theoretical Physicists

P. Arnold
E. Berger
G. Bodwin
R. Kauffman
R. Meng
D. Sinclair
D. Sivers
S. Vokos
K. C. Wang
A. White
C. Zachos

Engineers, Computer Scientists and Applied Scientists

E. Chojnacki
J. Dawson
T. Ekenberg
V. Guarino
D. Hill
N. Hill
J. Nasiatka
R. Noland
H. Rhude
J. Schlereth

Technical Support Staff

I. Ambats
L. Balka
H. Blair
W. Haberichter
D. Jankowski
T. Kasprzyk
R. Konecny
R. Laird
R. Rezmer
J Sheppard

Laboratory Graduate Participants

C. Ho
D. Keubel
M. Pundurs